TECHNICAL REPORT No. 28

THE EFFECT OF PRESTRAINING UNDER DIFFERENT STRESS STATES ON THE FRACTURE AND FLOW PROPERTIES OF 2S-O ALUMINUM

In Cooperation With
The Office of Naval Research, U. S. Navy
N6-ONR-273/I Project NR-031-049
SEPTEMBER 1953

An Investigation of

THE EFFECTS OF STRESS CONCENTRATION AND TRIAXIALITY ON THE PLASTIC FLOW OF METALS

Technical Report No. 28

THE EFFECT OF PRESTRAINING UNDER DIFFERENT STRESS STATES ON THE FRACTURE AND FLOW PROPERTIES OF 2S-O ALUMINUM

By

I. Rozalsky

Conducted By
METALS RESEARCH LABORATORY
DEPARTMENT OF METALLURGICAL ENGINEERING
CASE INSTITUTE OF TECHNOLOGY

In Cooperation With

OFFICE OF NAVAL RESEARCH, U.S. NAVY

Contract N6-ONR-273/I

Project NR-031-049

Cleveland, Ohio
October, 1953

METALS RESEARCH LABORATORY
DEPARTMENT OF METALLURGICAL ENGINEERING
CASE INSTITUTE OF TECHNOLOGY

Technical Report No. 28

THE EFFECT OF PRESTRAINING UNDER DIFFERENT STRESS STATES ON THE FRACTURE AND FLOW PROPERTIES OF 2S-O ALUMINUM

Written by

I. Rozalsky

Approved by

L. J. Ebert (JC)
L. J. Ebert
Assistant Task Order Director

W. M. Baldwin, Jr. (JC)
W. M. Baldwin, Jr.
Task Order Director

Distribution List for
Technical Report
No. 28

Copy No.____

Contract N6-onr-273/1 October, 1953 Project NR-031-049

Copy No.

1-2 Chief of Naval Research
Department of the Navy
Washington 25, D.C.
Attn: Code 423

3 Commanding Officer
Office of Naval Research
Branch Office
495 Summer Street
Boston 10, Massachusetts

4 Commanding Officer
Office of Naval Research
Branch Office
50 Church Street
New York 7, N.Y.

5 Commanding Officer
Office of Naval Research
Branch Office
The John Crerar Library Bldg.
10th Floor
86 E. Randolph Street
Chicago 11, Illinois

6 Commanding Officer
Office of Naval Research
Branch Office
801 Donahue Street
San Francisco 24, Calif.

7 Commanding Officer
Office of Naval Research
Branch Office
1030 Green Street
Pasadena, California

8 Assistant Naval Attache
for Research
London, England
U. S. Navy FPO #100
New York, N.Y.

9 Contract Administrator,
SE Area, Office of Naval Res.
Department of the Navy
Washington 25, D.C.
Att: Mr. K. F. Lynch

10-18 Director, Naval Res. Lab.
Washington 25, D.C.
Att: Technical Information
Officer

19 Dr. C. S. Smith
Institute for the Study of Metal
University of Chicago
Chicago, Illinois

20-21 University of California
Engineering Department
Berkeley, California
Att: Dr. J. E. Dorn
Dr. E. R. Parker

22 Professor F. A. Biberstein
Department of Mech. Engr.
Catholic University of America
Washington, D.C.

23 Professor W. Prager
School of Applied Mathematics
Brown University
Providence, Rhode Island

24 Dr. L. V. Griffis
Applied Mechanics Division
Armour Research Foundation
Chicago, Illinois

25 Dr. W. C. MacGregor
Dept. of Mech. Engr.
Massachusetts Inst. of Tech.
Cambridge, Massachusetts

26 Director
David Taylor Model Basin
Washington 7, D. C.

27 Armour Research Foundation
Metals Research Division
35 W. 33rd Street
Chicago, Illinois
Att: W. E. Mahin

28-29 Director, Naval Res. Laboratory
Washington 25, D. C.
Attn: Code 2500, Metallurgy
Code 2020, Tech. Library

30-33 Bureau of Aeronautics
Department of the Navy
Washington 25, D. C.
Attn: N. E. Promisel, AE-41(3)
Technical Library, TD-41(1)

34 Commanding Officer
Naval Air Material Center
Naval Base Station
Philadelphia, Penna.
Attn: Aeronautical Materials
Laboratory

35-38 Bureau of Ordnance
Department of the Navy
Washington 25, D. C.
Attn: Rex (3)
Technical Library AD3(1)

39 Superintendent, Naval Gun Factory
Washington 20, D. C.
Attn: Metallurgical Lab IN910

40 Commanding Officer
U. S. Naval Ordnance Laboratory
White Oaks, Maryland

41 Commanding Officer
U. S. Naval Ordnance Test Station
Inyokern, California

42-45 Bureau of Ships
Department of the Navy
Washington 25, D. C.
Attn: Code 343 (3)
Code 337L, Tech. Lib. (1)

46 U. S. Naval Engineering
Experiment Station
Annapolis, Maryland
Attn: Metals Laboratory

47 Director, Materials Laboratory
Building 291
New York Naval Shipyard
Brooklyn 1, New York
Attn: Code 907

48 Bureau of Yards and Docks
Department of the Navy
Washington 25, D. C.
Attn: Research & Standards Div.

ARMY

49 Chief of Staff, U. S. Army
The Pentagon
Washington 25, D. C.
Attn: Director of Research &
Development

50-52 Office of Chief of Ordnance
Research & Development Service
Department of the Army
Washington 25, D. C.
Attn: ORDTB

53 Commanding Officer
Watertown Arsenal
Watertown, Massachusetts
Attn: Laboratory

54 Office of Chief of Engineers
Department of the Army
Washington 25, D. C.
Attn: Research & Development Br.

AIR FORCES

55 U. S. Air Forces
Research and Development Div.
The Pentagon
Washington 25, D. C.

56-57 Air Materiel Command
Wright-Patterson Air Force Base
Dayton, Ohio
Attn: Materials Laboratory
MCREXM

OTHER GOVERNMENT AGENCIES

58 Atomic Energy Commission
Division of Research
Metallurgical Branch
Washington 25, D. C.

59 National Bureau of Standards
Washington 25, D. C.
Attn: Physical Metallurgy Division
Technical Library

60 National Advisory Committee
for Aeronautics
1724 F Street, N. W.
Washington 25, D. C.

61 Research & Development Board
Committee on Basic Physical
Sciences
The Pentagon
Washington 25, D. C.
Attn: Metallurgy Panel

62 Commanding Officer
Naval Proving Grounds
Dahlgren, Virginia
Attn: Laboratory Division

63 Dr. Henry Eyring
School of Mines & Mineral Ind.
University of Utah
Salt Lake City, Utah

64 Dr. Finn Jonassen
National Research Council
2101 Constitution Avenue, N. W.
Washington 25, D. C.

65 Dr. D. S. Clark
Department of Mech. Engr.
California Institute of Tech.
Pasadena, California

66-67 University of Illinois
Urbana, Illinois
Att: Dr. N. M. Newmark
Dr. T. J. Dolan

68 Dr. R. M. Brick
Department of Metallurgy
University of Pennsylvania
Philadelphia, Penna.

69 Bureau of Ships
Department of the Navy
Washington 25, D. C.
Attn: Code 692

70 Professor M. Cohen
Department of Metallurgy
Massachusetts Inst. of Tech.
Cambridge 39, Mass.

71 General Electric Company
Research Laboratories
Schenectady, New York
Attn: J. H. Hollomon

72 Dr. Robert Maddin
Department of Mech. Engr.
Johns Hopkins University
Baltimore, Maryland

73 Dr. R. F. Mehl
Director of Metals Research Lab.
Carnegie Institute of Tech.
Pittsburgh, Penna.

74 Brookhaven National Laboratory
Information & Publication Div.
Documents Section
Upton, New York
Attn: Miss Mary E. Waisman

75 Carbide and Carbon Chemicals Div.
Plant Records Department
Central Files (K-25)
P. O. Box P
Oak Ridge, Tennessee

76 Carbide and Carbon Chemicals Div.
Central Reports & Information
Office
P. O. Box P (Y-12)
Oak Ridge, Tennessee

77 General Electric Company
Technical Services Division
Technical Information Group
P. O. Box 100
Richland, Washington
Attn: Miss M. G. Freidank

78 Iowa State College
P. O. Box 14A, Station A
Ames, Iowa
Attn: Dr. F. H. Spedding

79 Knolls Atomic Power Laboratory
P. O. Box 1072
Schenectady, New York
Attn: Document Librarian

80 Los Alamos Scientific Lab.
P. O. Box 1663
Los Alamos, New Mexico
Attn: Document Custodian

81 U. S. Atomic Energy Commission
New York Operations Office
P. O. Box 30, Ansonia Station
New York 23, N. Y.
Attn: Division of Tech. Inf.
and Declassification Service

82 Oak Ridge National Laboratory
P. O. Box P
Oak Ridge, Tennessee
Attn: Central Files

83 Sandia Corporation
Sandia Base
Classified Document Division
Albuquerque, New Mexico
Attn: Mr. Dale N. Evans

84 U. S. Atomic Energy Commission
Library Branch, Tech. Inf.
Service, ORE
P. O. Box E
Oak Ridge, Tennessee

85 University of California
Radiation Laboratory
Information Division
Room 128, Building 50
Berkeley, California
Attn: Dr. R. K. Wakerling

86 Westinghouse Electric Corp.
Atomic Power Division
P. O. Box 1468
Pittsburgh 30, Penna.
Attn: Librarian

87 Dr. M. Gensamer
91 Columbia University
New York, N. Y.

88 Dr. W. M. Baldwin, Jr.
Case Institute of Technology

89 Dean Elmer Hutchisson
Case Institute of Technology

90 Dr. A. R. Troiano
Case Institute of Technology

91 Mr. L. J. Ebert
Case Institute of Technology

92 Mr. E. J. Ripling
Case Institute of Technology

93 Mr. L. J. Klingler
Case Institute of Technology

94 Metals Research Laboratory
Case Institute of Technology
(File Copy)

THE EFFECT OF PRESTRAINING UNDER DIFFERENT STRESS STATES ON THE FRACTURE AND FLOW PROPERTIES OF 2S-O ALUMINUM *

By

I. Rozalsky **

ABSTRACT

The effects of prestrain under conditions of different stress states but identical strain states upon the fracture and flow properties in tension were obtained for commercially pure (2S-O) aluminum.

For prestrains of the same magnitude a prestrain stress state of simple compression results in a higher retained tensile ductility than does a prestrain stress state of biaxial tension. Also a change in prestrain stress state from simple compression to biaxial tension influences the shape of the fracture stress versus prestrain curve but does not affect the shape of the yield strength versus prestrain curve.

- - - - - - - - -

* This paper is based upon a portion of a research program conducted in the Metals Research Laboratory, Department of Metallurgical Engineering, Case Institute of Technology, Cleveland, Ohio in cooperation with the Office of Naval Research, U. S. Navy.

** Research Associate, Metals Research Laboratory, Case Institute of Technology.

INTRODUCTION

The object of this investigation was a correlation of the prestrain effects produced under conditions of different stress states but identical strain states upon the tensile fracture and flow properties of 2S-O aluminum.

Fig. 1* summarizes some of the possible types of plastic strains or prestrains that may be followed by a tensile test.

Tensile prestrain in the same direction as that of the subsequent tensile test may be produced under prestrain conditions of different stress states but identical strain states.

The conditions represented by Fig. 1a, the prestrain stress state of simple tension, have been studied by Liu and Sachs (1)** for 24ST aluminum and by Ripling and Baldwin (2) and McAdam and his associates (3) for steel.

Bridgman (4) considered the conditions represented by Fig. 1b, the prestrain stress state of biaxial compression, in his studies of a number of alloys.

The prestrain stress state of "cross-compression"*** represented

---

* The subscripts a, b, and c for each stress (s) and strain (ε) may apply interchangeably to any of the three principal directions.

** Numbers in parentheses refer to the Bibliography at the end of this paper.

*** Compressive prestrain in one principal direction followed by testing in one of the other principal directions (90 degrees removed from the prestrain direction). The "cross-compression" results in a tensile prestrain in the test direction.

by Fig. 1c and 1d was considered in this paper as another possible means of obtaining tensile prestrain.

Compressive prestrain in the same direction as that of the subsequent tensile test may also be produced under conditions of different stress states but identical strain states.

The conditions represented by Fig. 1e, the prestrain stress state of simple compression, were studied by Liu and Sachs for 24ST aluminum (1), Ripling and Baldwin (2), McAdam (3) and Koerber and his coworkers (5) for steel.

The prestrain stress state of biaxial tension represented by Fig. 1f was considered in this research as another means of obtaining compressive prestrain in the same direction as that of the subsequent tensile test.

MATERIAL AND PROCEDURE

The different prestraining conditions were carried out on specimens cut from a 10 foot by 4 foot by 3/4 inch 2S aluminum plate and annealed at 650°F for 30 minutes.* The methods by which the tests were conducted are described below:

Final Tensile Test

These specimens were of the dimensions shown in Fig. 2 except for specimens taken in the normal direction of the plate after compressive prestrain in the normal direction. Under these conditions, see Fig. 1e

- - - - - - - -

* In the fully annealed condition the 2S aluminum is designated as 2S-O aluminum.

and 1f, the total length of the tensile test specimen was necessarily decreased; however, the specimen diameter of 0.150 inch was retained.

Each tensile test was made with a crosshead speed of approximately 0.04 inch per minute, with all tests including the prestrains being made at room temperature. Concentricity of loading during the tensile testing operation was ensured by the use of a specially constructed fixture (6).

Prestrain According to Fig. 1a

The type of specimen used for simple tensile prestrain was of the shape shown in Fig. 2. It was not considered necessary to re-machine these specimens prior to their being tested in tension. Prestrains of this type and subsequent tensile tests were made for each of the three principal directions, i.e., the longitudinal (rolling), transverse, and normal directions of the aluminum plate. The direction of the tensile prestrain was the same as the direction of the subsequent tensile test.

Prestrain According to Figs. 1c and 1d

The type of specimen used for cross-compressive prestrain was a rectangular parallelepiped of the dimensions 0.72 inch by 0.50 inch by 0.50 inch or 0.72 inch by 2.00 inch by 2.00 inch. The 0.72 inch dimension was in the normal direction of the plate, the dimensions in the longitudinal and transverse directions being determined by the direction of the subsequent tensile test and the magnitude of prestrain.

Specimens were prestrained by compressing them between two flat parallel plates in a tensile test machine. A commercial preparation of molybdenum sulfide was used as a lubricant on the plates to decrease

friction between the plates and the specimen bases. This technique was also used for simple compressive prestrain, see Fig. 1e.

For each of the three test directions two sets of data were obtained by means of cross-compressive prestrain, e.g., for tests in the normal direction, it was possible to prestrain by compression in either the longitudinal or transverse direction to obtain a tensile prestrain in the normal direction.

Prestrain According to Fig. 1e.

The type of specimen used for prestraining in simple compression was a cylinder, the axis of which was parallel to the direction of compression and the test direction. Those taken in the normal direction of the plate were 0.72 inch in height and 0.50 inch in diameter. The maximum amount of prestrain was ε_p* = -0.60; greater prestrains reduced the length of the subsequent tensile test specimens to an impractical point. Those taken in the longitudinal and transverse directions were of two sizes:

0.75 inch in height and 0.50 inch in diameter for compressive prestrains less than $\varepsilon_p = -0.60$, and

2.00 inch in height and 0.75 inch** in diameter for compressive prestrains greater than $\varepsilon_p = -0.60$.

The maximum length of the tensile test specimen taken in the normal direction that could be machined from the plate after heavy compressive

---

* $\varepsilon_p = \ln \frac{\text{Original Area}}{\text{Area after Prestrain}}$

** Narrow flats were left on the cylindrical surfaces of these specimens for the plate thickness was only 0.72 inch, see Fig. 4.

prestrain in the normal direction, according to Fig. 1e or 1f, was shorter the greater the prestrain. It was observed that the effect of variation in gage length upon the fracture and flow properties of the 2S-O aluminum was not significant, except for the yield strength of specimens of exceedingly short gage length.

The aluminum plate used in this investigation was anisotropic as may be seen in Fig. 3 and 4 by the oval cross-section which originally circular specimens assumed when compressed.

Prestrain According to Fig. 1f

Prestraining in biaxial tension was effected by bulging the 2S-O aluminum plate by hydraulic means on a 1,000,000 pound hold-down press. While thin sheet has previously been bulged in such presses (7) (8), the bulging of thick sheet or plate introduces two difficulties:

(a) The bend stresses at the periphery of the bulge are such as to destroy a simple biaxial stress state for some distance in from the edge. Consequently, as large a diameter die (6 inch diameter with a specimen of 10 inch by 10 inch surface dimensions) as could be handled by the press was used. Tensile test specimens were taken from the center (pole) of each dome (bulge) normal to the surface of the plate*.

(b) Even at the pole of the dome a uniform biaxial strain state did not exist from the inside surface to the outside surface as was evidenced

- - - - - - - -

* Actually a simple biaxial stress state (stresses in the plane of the sheet only) is not achieved in the case of bulging thick plate since here the hydraulic pressure develops some slight stress normal to the plane of the sheet.

by strains measured from 20-lines-to-the-inch grids photographically applied (9) to both the outside and inside surfaces.

After bulging, strain distributions on the top and bottom surfaces of each bulge were plotted, Fig. 5, 6, and 7, for the portion of the bulge in the vicinity of the pole.

The strains were measured from the pole, see Fig. 5, in the longitudinal direction of the plate at the top and bottom surfaces (e_{LT} and e_{LB}, respectively) and in the transverse direction of the plate at the top and bottom surfaces (e_{TT} and e_{TB}, respectively) of the bulge. The bottom surface of the bulge was denoted to be the surface in contact with the oil during the bulging operation.

The first plate was bulged until fracture occurred. By extrapolation of Thielsch's data for the hydraulic pressure required for fracture versus thickness of sheet for 2S-O aluminum (10), it was determined that an approximate pressure of 6500 psi would be required to fracture 3/4 inch plate under conditions of balanced* biaxial tension by means of hydraulic bulging. Actually, it was experimentally determined that a pressure of 7500 psi was required. The difference in hydraulic pressure was perhaps due in part to the slight triaxiality in stress state involved in the bulging of the plate.

No tensile test specimens were taken from this bulge which fractured under hydraulic pressure, because of the excessive non-uniformity of strain distribution. More aluminum plates were bulged at successively lower

- - - - - - - -

* Using circular bulging die.

pressures, and from one specimen, see Fig. 5a, to nine specimens, see Fig. 7b, were taken from the pole of each bulge, the number of specimens depending upon the uniformity of strain in the vicinity of the pole. Each specimen was cut from the bulge so that its axis was perpendicular to the top bulge surface.

Compressive prestrain in each of these specimens was computed (a) from thickness measurements made with pointed micrometers and (b) from the average strains in the plane of the plate taken on both the inside and outside surfaces by the assumption of constancy of volume,

$$\varepsilon_1 + \varepsilon_2 + \varepsilon_3 = 0$$

ε_1 being the longitudinal strain, ε_2 the transverse strain and ε_3 the normal strain. The results obtained by both methods for each specimen were almost identical.

A considerable strain gradient existed between the top and bottom surfaces of each bulge, see Figs. 5, 6, and 7, and concomitantly, between the bases of the tensile test specimens cut from the pole of each bulge. For low hydraulic bulging pressures, the strains in the longitudinal and transverse directions were compressive* at the bottom surface and tensile at the top surface of the bulge, however, for high pressures, the strains at the top and bottom surfaces were both tensile but varied greatly in magnitude.

To determine the strain gradient throughout the thickness, Knoop hardness traverses were made on specimens cut from the poles of the bulges,

- - - - - - - -

* The apparently anamalous compressive strains cannot be explained by the author at this time; however, their explanation may lie in the realm of bulge mechanics.

Fig. 8. The variation in Knoop hardness was essentially linear with respect to thickness, even after taking into account the minima in these curves where a transition from compressive to tensile strains occurred at some distance from the bottom surface of the bulge. The hardness was assumed proportional to the strain, thus the strain at any depth could be obtained. Hence, although some of the tensile test specimens did not fracture at the exact center of the gage length, the magnitude of the prestrain at the point of fracture in the tensile test specimen could be determined.

RESULTS

The effect of prestrain (ε_p) upon various fracture and flow properties of 2S-O aluminum in tension are represented in Figs. 9 to 24. The fracture properties determined were the retained ductility (ε_f)* and the fracture stress (S_f)**. The only flow property investigated was the yield strength (0.2% offset).

Fracture Properties

Retained Ductility

Plots of retained tensile ductility versus prestrain for prestrain stress states of simple compression ($\varepsilon_p < 0$), simple tension ($\varepsilon_p > 0$), and cross-compression ($\varepsilon_p > 0$) are shown in Fig. 9, 10 and 11 for specimens prestrained

---

$$*\varepsilon_f = \ln \frac{\text{Area After Prestrain}}{\text{Final Area}} = \frac{A_p}{A_f}$$

$$**S_f = \frac{\text{Load at Fracture}}{\text{Area at fracture}}$$

and tested in the normal, longitudinal and transverse directions, respectively.

For each of the three test directions the curves for the prestrain stress states of simple tension and cross-compression appear to coincide in a straight line of 45 degree slope.

However, for tests taken in the normal direction, Fig. 9, for large cross-compressive prestrains in the longitudinal and transverse directions, there appears to be a tendency for deviation from the 45 degree line in a manner analagous to the curve for biaxial compression, see Fig. 12. It was not possible to justify this tendency for deviation from the 45 degree line, because of experimental difficulties, e.g., prestrain specimen size limitation in the normal direction and buckling tendencies in prestraining restricted the magnitude of the prestrains to those shown in Fig. 9. In this paper the curves for cross-compressive prestrain will be assumed to lie along a line of 45 degree slope for all three test directions as shown in Figs. 9, 10 and 11.

In these plots the following should be noted for each test direction:

The continuous nature of each of the curves from tensile prestrains ($\varepsilon_p > 0$) through zero prestrain ($\varepsilon_p = 0$) to compressive prestrains ($\varepsilon_p < 0$); the maximum in the curve at a simple compressive prestrain of small magnitude; and the subsequent decrease in retained tensile ductility (ε_f) at larger compressive prestrains. These features have also been observed in other investigations (1) (2).

A plot of the retained tensile ductility versus prestrain under a prestrain stress state of biaxial tension and a schematic curve of the expected

retained tensile ductility (4) versus prestrain under the stress state of biaxial compression are shown in Fig. 12. For compressive prestrain (biaxial tension), the curve is a straight line of very steep slope, e.g., the retained ductility decreases very rapidly with increasing compressive prestrain. For tensile prestrain (biaxial compression), the curve has a smaller slope than the curve for simple tension (45 degrees) after exceeding some critical magnitude of prestrain (4).

The curves in Fig. 9, 10 and 11 were combined with similar curves for 24S-T4 aluminum (1) and SAE 1340 steel* (2) in Fig. 13.

A comparison of the unworked ductilities of 2S-O aluminum in each of the three directions of the plate shows that the ductility in the normal direction is somewhat greater than that in either the longitudinal or transverse direction. At large compressive prestrains, however, the retained ductility is greater for the longitudinal and transverse directions than for the normal direction. Of course, for the tensile prestrains, the ductility in the normal direction for any magnitude of prestrain is greater than that in the longitudinal or transverse direction because of the relationship between the unworked ductilities ($\varepsilon_p = 0$) in the three directions.

The general shapes of the curves for 24S-T4 aluminum and SAE 1340 steel are similar to those for simple tensile or compressive prestrain for 2S-O aluminum.

Because of the much lower unworked ductilities of 24S-T4 aluminum and SAE 1340 steel in comparison with that of 2S-O aluminum, the plots in

- - - - - - - -

* For specimens taken in the longitudinal direction of round bar stock.

Fig. 13 are transposed to Fig. 14 where the ratio of retained ductility to unworked ductility is plotted versus the ratio of prestrain to unworked ductility.

The curve for SAE 1340 steel is considerably higher than the other curves, whereas the curve for 24S-T4 aluminum approximates somewhat the curve for 2S-O aluminum prestrained and tested in the longitudinal direction.

For comparison purposes Fig. 15 was obtained by combining the curves in Fig. 12 with the curve for the prestrain stress state of simple compression in the normal direction in Fig. 9.

Fracture Stress

Plots of tensile fracture stress versus prestrain under conditions of different stress states are shown for the normal direction, Fig. 16, the longitudinal direction, Fig. 17, and the transverse direction, Fig. 18.

For each of the three principal directions for prestrain in simple tension, the curve appears to be a horizontal line; however, for prestrain stress states of simple compression and "cross-compression", each of the tensile fracture stress curves exhibits a minimum for each of the three test directions.

Fig. 19 shows plots of tensile fracture stress versus compressive prestrain for the prestrain stress state of simple compression in each of the three principal directions and for the prestrain stress state of biaxial tension in the normal direction. Also included is the curve for 24S-T4 aluminum (1). The curves for simple compressive prestrain for each of

three directions in the 2S-O aluminum plate are similar in that each exhibits a minimum at a relatively low magnitude of prestrain and then rises; however, the curves for the longitudinal and transverse directions do show a tendency to flatten out at higher prestrains at a fracture stress of the order of magnitude of 50,000 psi. The curve for the prestrain stress state of biaxial tension for 2S-O aluminum differs in that it is a straight line of steep slope with no minimum and no propensity towards flattening out. The curve for 24S-T4 aluminum is a straight line of gentle slope.

The Effect of Prestrain Upon Flow Properties

Yield Strength

Plots of yield strength in tension versus prestrain for different prestrain stress states are shown for the normal direction, Fig. 20; the longitudinal direction Fig. 21; and the transverse direction, Fig. 22. For a given principal direction, there are but slight differences in the yield strength curves for the various prestrain stress states.

Plots of yield strength in tension versus compressive prestrain for the prestrain stress state of simple compression in each of the three principal directions and for the prestrain stress state of biaxial tension in the normal direction are shown in Fig. 23. Also included is the curve for 24S-T4 aluminum (1). The curves for 2S-O aluminum for simple compression in the three principal directions are all quite similar. This similarity can also be shown for the other prestrain stress states. Liu's curve is of course much higher than those for 2S-O aluminum, has a minimum at a very small value of prestrain, and has a much steeper slope at prestrains of small magnitude.

DISCUSSION OF RESULTS

Prestraining in Biaxial Tension

It is apparent in Fig. 5, 6 and 7 that the strain anisotropy in the bulge at the vicinity of the pole of the bulge is strain dependent; i.e., the greater the longitudinal and transverse strains in the bulge surfaces, the greater is the strain anisotropy.

The Effect of Prestrain upon the Retained Ductility

The inherent scatter of the data for the unworked ductility for 2S-O aluminum in each of the three directions of the plate should be noted in Figs. 9, 10 and 11. This characteristic scatter in unworked ductility is an implicit factor in the scatter of the retained ductility versus prestrain data for the above curves.

The relatively large scatter in the retained ductility versus prestrain data for the stress state of biaxial tension, Fig. 12, was probably caused by a combination of variations in the previously mentioned bend stresses and by the plate anisotropy. The trend of the data might have been more apparent if it had been possible to obtain larger compressive prestrains by means of biaxial tension. This condition was not possible with the material and equipment used in this investigation.

The greater unworked ductility in the normal direction than in the longitudinal direction of the 2S-O aluminum plate appears anomalous when compared with the results in the published literature (11). The discrepancy cannot be explained at this time.

The differences between the curves for retained tensile ductility versus

prestrain in simple compression in the normal direction and in biaxial tension, Fig. 15, seem to be of fundamental significance. The unknown mechanism which causes an increase in retained tensile ductility for small compressive prestrains for a prestrain stress state of simple compression appears to be inoperative for a prestrain stress state of balanced biaxial tension.

The absence of a discontinuity in the prestrain curve from simple compressive to simple tensile prestrain in Fig. 13 possibly indicates that the small increase in retained ductility for small values of compressive prestrain has only a slight effect upon the fracture mechanism in tension.

A change in prestrain stress state from simple tension to "cross-compression" does not affect the retained tensile ductility, see Fig. 9, 10 and 11, but a change in prestrain stress state to simple compression or biaxial tension, Fig. 15, modifies the retained tensile ductility curve.

From Fig. 1 the prestrain stress state of cross-compression is apparently intermediate between simple tension and biaxial compression. The results, however, indicate that for each of the three test directions the curve for retained tensile ductility versus prestrain in cross-compression, Figs. 9, 10 and 11, coincides with the curve for simple tension, rather than lying somewhere between the curves for prestrain in simple tension and biaxial compression, Fig. 15.

Fracture Stress

Although the retained ductility and fracture stress are both considered

to be fracture properties, the change in prestrain stress state from simple tension to "cross-compression" (for both, $\varepsilon_p > 0$) caused no change in the retained tensile ductility curve, Figs. 9, 10 and 11, but caused a change in the shape of the tensile fracture stress curve, Figs. 16, 17 and 18.

These results should be considered from the point of view that the fracture stress is not a simple phenomenon. The fracture stress of a metal depends upon the ductility, the strain hardening rate and the yield strength of the metal. The interrelations between the above variables and considerations of their relative magnitudes could certainly produce minima in those curves for tensile fracture ductility when the prestrain stress state is changed from one of simple tension to simple compression or "cross-compression", see Figs. 16, 17 and 18, or change the slope of the fracture stress curve from a horizontal line for a prestrain stress state of simple tension to a straight line of steep slope for a prestrain stress state of biaxial tension, see Fig. 16.

The curves for prestrain in simple compression for the three directions of the 2S-O aluminum plate exhibit certain similarities, see Fig. 19. There is a minimum in each of these curves at a small value of compressive prestrain. Then the curves for the longitudinal and transverse directions rise, flattening out at larger prestrains at fracture stress values of about 50,000 psi. It seems possible to expect that the curve for the normal direction would also have flattened out after rising from the minimum, had it been possible to obtain larger prestrains in the normal direction.

Liu's curve for 24S-T4 aluminum is of different shape from the above

curves for 2S-O aluminum. The difference may be explained by the large difference in ductility between 2S-O and 24S-T4 aluminum. Koerber (5) found that the tensile fracture stress for a mild steel consistently decreased with increasing compressive prestrain. But McAdam (3) reported that with increasing compressive prestrain, the tensile fracture stress of an annealed chromium steel first decreased to a minimum and then increased continuously. Complex curves for fracture stress versus prestrain were obtained by Backofen and his associates (12) under conditions of prestrain in torsion and testing in tension. It is possible that a difference between the stress state in prestraining and in testing tends to complicate the horizontal curve expected when the stress states for prestrain and testing are of the same type.

The curve for fracture stress versus prestrain in balanced biaxial tension is significantly different from that for simple compressive prestrain in the normal direction, Fig. 19. Apparently, the effect of the balanced biaxial tensile prestrain is to mask completely those characteristics present in the curve for simple compressive prestrain and to cause only a rapid linear decrease in fracture stress with increasing compressive prestrain.

Yield Strength

The evident proximity of the curves for all prestrain stress states, see Figs. 20 to 23, indicates that a difference in prestrain stress state has no significant influence upon the effect of prestrain on the yield strength in tension.

CONCLUSIONS

The fracture properties (stress and strain) of 2S-O aluminum depend not only upon the nature and magnitude of the prestrain, but also upon the stress state under which a given prestrain is effected, see Fig. 24.

Thus, for example, for each test direction for compressive prestrains of the same magnitude, a prestrain stress state of simple compression resulted in a higher retained tensile ductility than did a prestrain stress state of biaxial tension.

For tensile prestrains of the same magnitude (after a critical amount of prestrain) a prestrain stress state of biaxial compression resulted in a higher retained tensile ductility than did a prestrain stress state of simple tension.

However, for tensile prestrains of the same magnitude, a prestrain stress state of simple tension resulted in the same retained tensile ductility as did a prestrain stress state of cross-compression.

For compressive prestrains of the same magnitude, a prestrain stress state of simple compression resulted in a higher tensile fracture stress than did a prestrain stress state of biaxial tension.

The shapes of the curves obtained for tensile fracture stress versus prestrain differed considerably when the prestrain stress state was varied.

No significant changes in the tensile yield strength versus prestrain curves were obtained by variations in the prestrain stress states.

ACKNOWLEDGMENTS

This work was conducted in cooperation with the Office of Naval Research, U. S. Navy. The aid and advice of Dr. W. M. Baldwin Jr., Mr. L. J. Ebert, Dr. E. J. Ripling and other members of the Metals Research Laboratory are greatly appreciated.

BIBLIOGRAPHY

(1) S. I. Liu and G. Sachs, The Flow and Fracture Characteristics of the Aluminum Alloy 24ST after Alternating Tension and Compression, Metals Tech., Vol. 15 (June, 1948), TP2392.

(2) E. J. Ripling and W. M. Baldwin, Jr., Overcoming Rheotropic Brittleness: Precompression Versus Pretension, Trans. Am. Soc. Metals, Vol. 44 (1952), p. 1047-1054.

(3) D. J. McAdam, Jr., G. W. Geil and W. D. Jenkins, Influence of Plastic Extension and Compression on the Fracture Stress of Metals, Trans. A.S.T.M., Vol 47 (1947), p. 554-574.

(4) P. W. Bridgman, Studies in Large Plastic Flow and Fracture, McGraw-Hill (1952), p. 293-310.

(5) F. Koerber, A. Eichinger and R. Moeller, The Behavior under Tensile Stress of Metals Deformed by Compression, Mitt. Kaiser-Wilhelm Inst. Eisenforschung, Duesseldorf, Vol. 26 (1943), p. 71-88.

(6) G. Sachs, J. D. Lubahn and L. J. Ebert, Notched Bar Tensile Tests on Heat Treated Low Alloy Steels, Trans. Am. Soc. Metals, Vol. 31 (1943), p. 136-160.

(7) G. Sachs, G. Espey, and G. B. Kasik, Circular Bulging of Aluminum Alloy Sheet at Room and Elevated Temperatures, Trans. Am. Soc. Mech. Engrs., Vol. 68 (1946), p. 161-173.

(8) W. T. Lankford, A. R. Low and M. Gensamer, The Plastic Flow of Aluminum Alloy Sheet under Combined Loads, Trans. A.I.M.E., Vol. 171 (1947), p. 574-604.

(9) W. F. Brown, Jr. and M. H. Jones, Strain Analysis by Photogrid Method, Iron Age, Vol. 153 (Sept. 12, 1946), p. 50-55.

(10) H. Thielsch, Bulge Testing of Sheet Metal, Metal Progress, Vol. 56 (July, 1949), p. 86-88.

(11) L. J. Klingler and G. Sachs, Fracturing Characteristics of Aluminum-Alloy Plate, Jour. of the Aero. Sciences, Vol. 15, No. 12 (Dec. 1948), p. 731-734.

(12) W. A. Backofen, B. B. Hundy and J. Wulff, The Ductile Fracture of Metals, Tech. Report No. 3, O.N.R. Contr. N5ori-07841, Project No. NR 031-356 (July 30, 1951), p. 7-8.

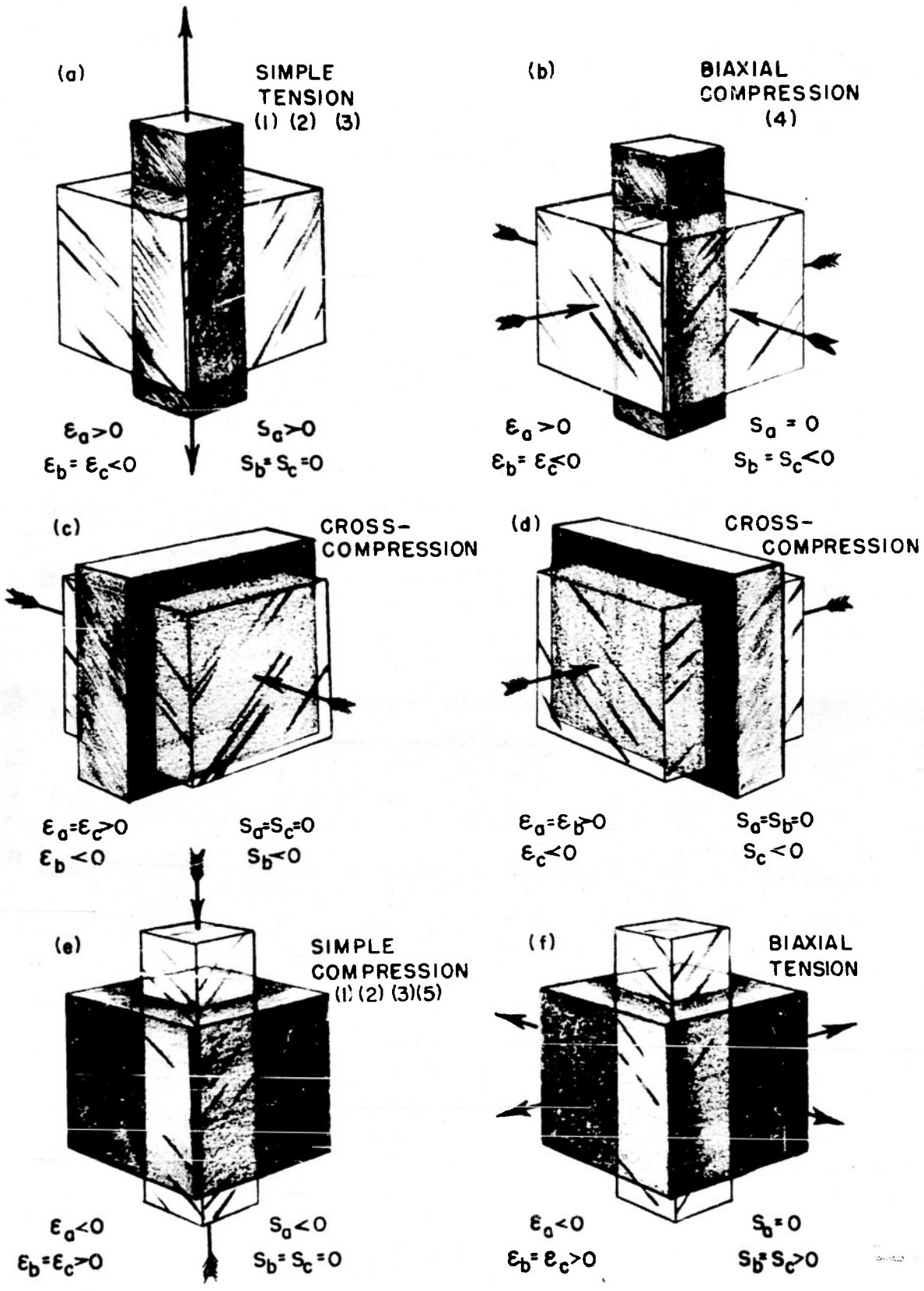

FIG. 1 : VARIOUS PRESTRAIN STRESS AND STRAIN STATES UNDER ISOTROPIC CONDITIONS. CLEAR BLOCKS INDICATE SHAPE BEFORE PRESTRAINING.

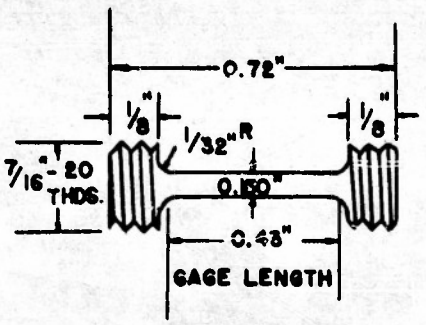

Fig.2: TENSILE TEST SPECIMEN

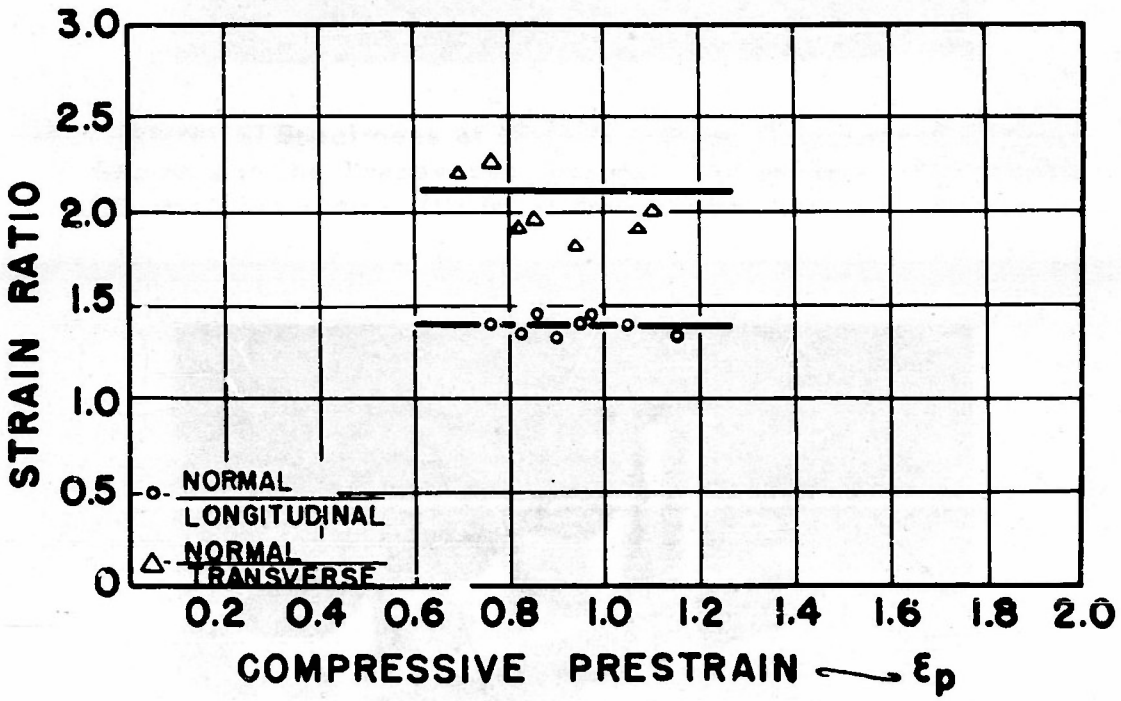

Fig. 3: DEPENDENCE OF STRAIN ANISOTROPY UPON COMPRESSIVE PRESTRAIN IN 3/4 INCH THICK 2S-O ALUMINUM PLATE.

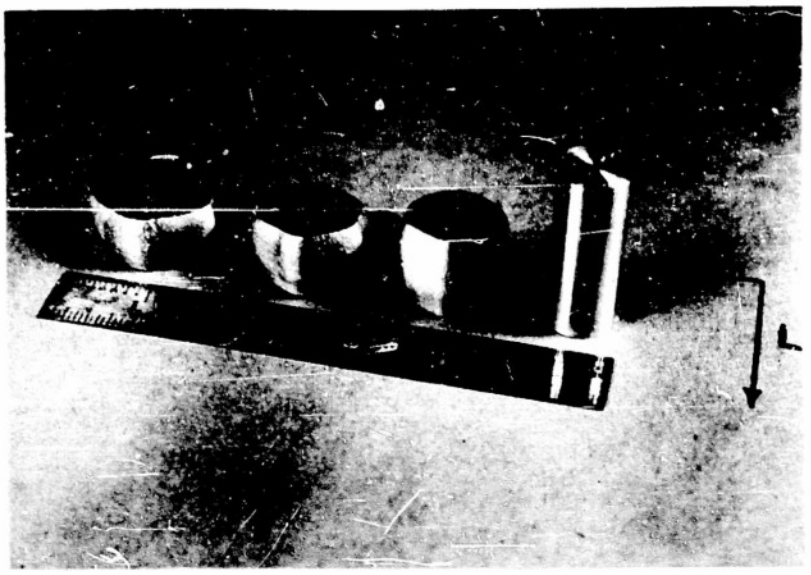

(a) Cylindrical Specimens of 2S-O Aluminum Compressed Various Amounts in the Transverse Direction of the Plate. The Normal (N) and Longitudinal (L) Directions of the Plate are Shown.

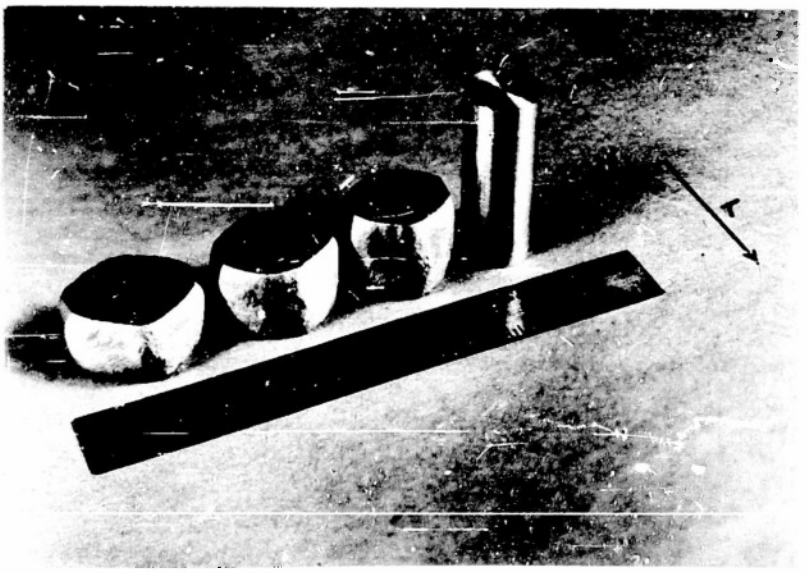

(b) Cylindrical Specimens of 2S-O Aluminum Compressed Various Amounts in the Longitudinal (Rolling) Direction of the Plate. The Normal (N) and Transverse (T) Directions are Shown.

FIG. 4: - PLATE ANISOTROPY AS EVIDENCED BY SPECIMENS PRESTRAINED IN SIMPLE COMPRESSION.

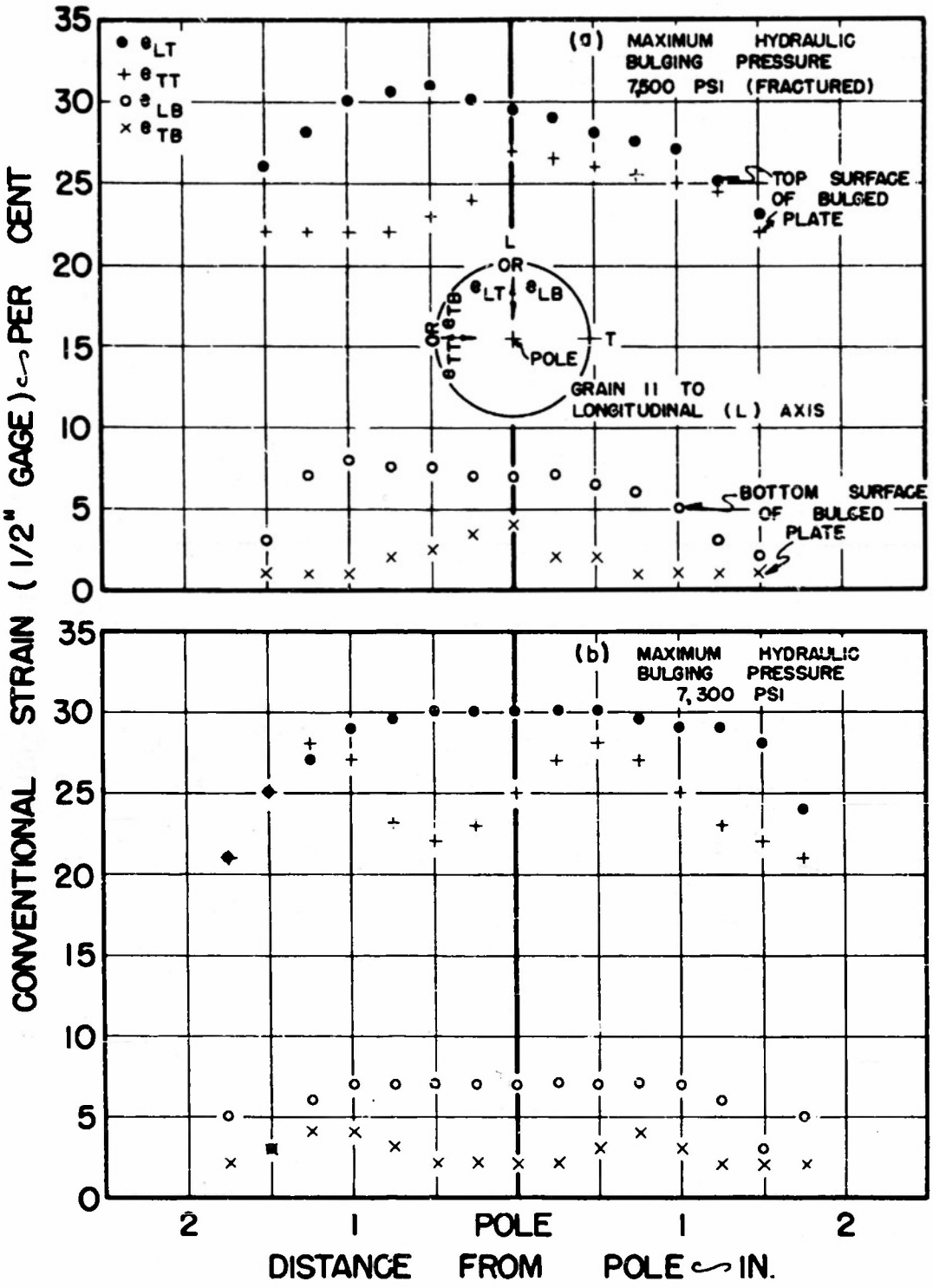

FIG. 5 : LONGITUDINAL AND TRANSVERSE STRAIN DISTRIBUTIONS FOR HYDRAULIC CIRCULAR BULGES OF 3/4" 2S-O ALUMINUM PLATE.

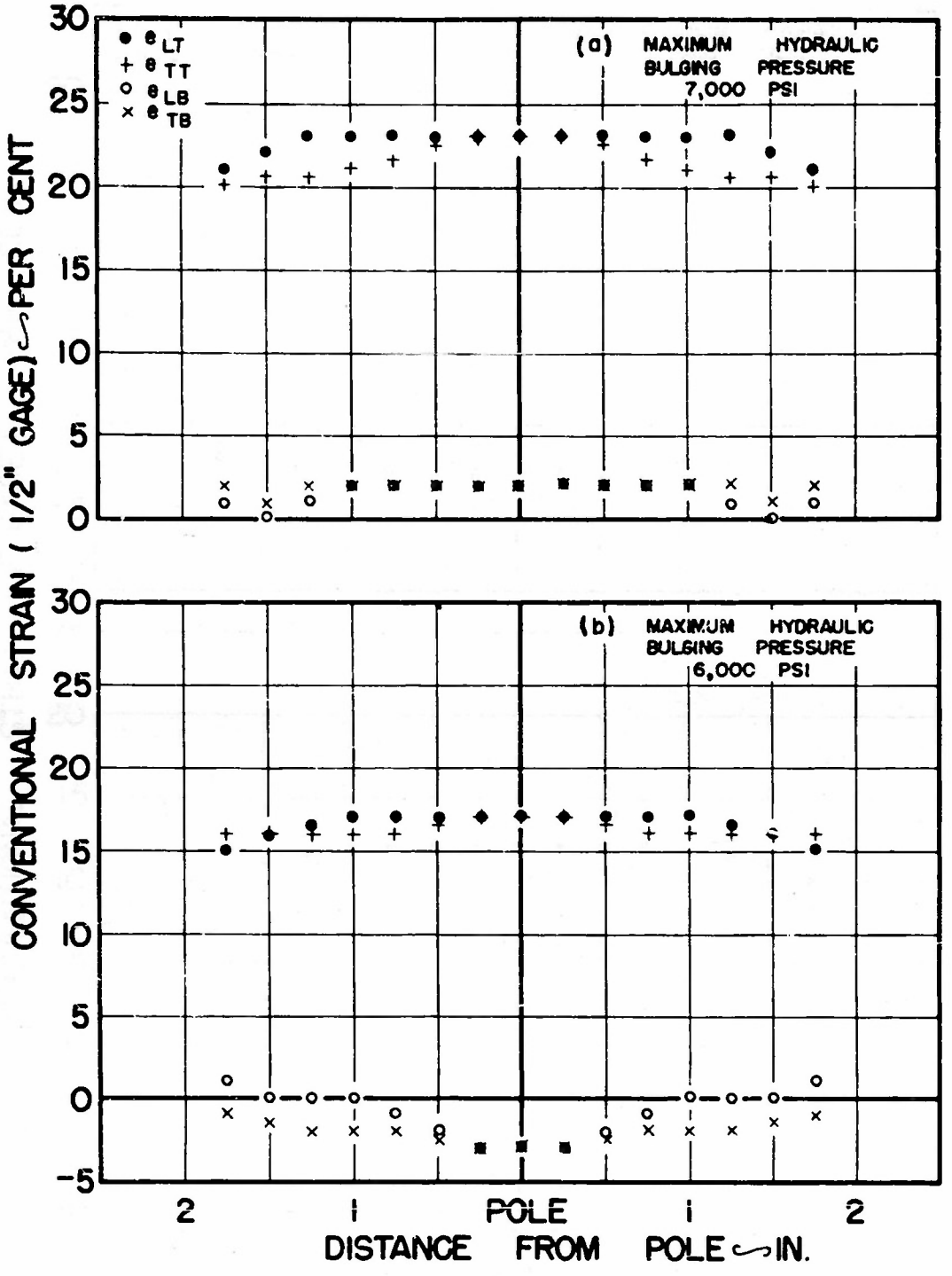

FIG. 6 : LONGITUDINAL AND TRANSVERSE STRAIN DISTRIBUTIONS FOR HYDRAULIC CIRCULAR BULGES OF 3/4" 2S-O ALUMINUM PLATE.

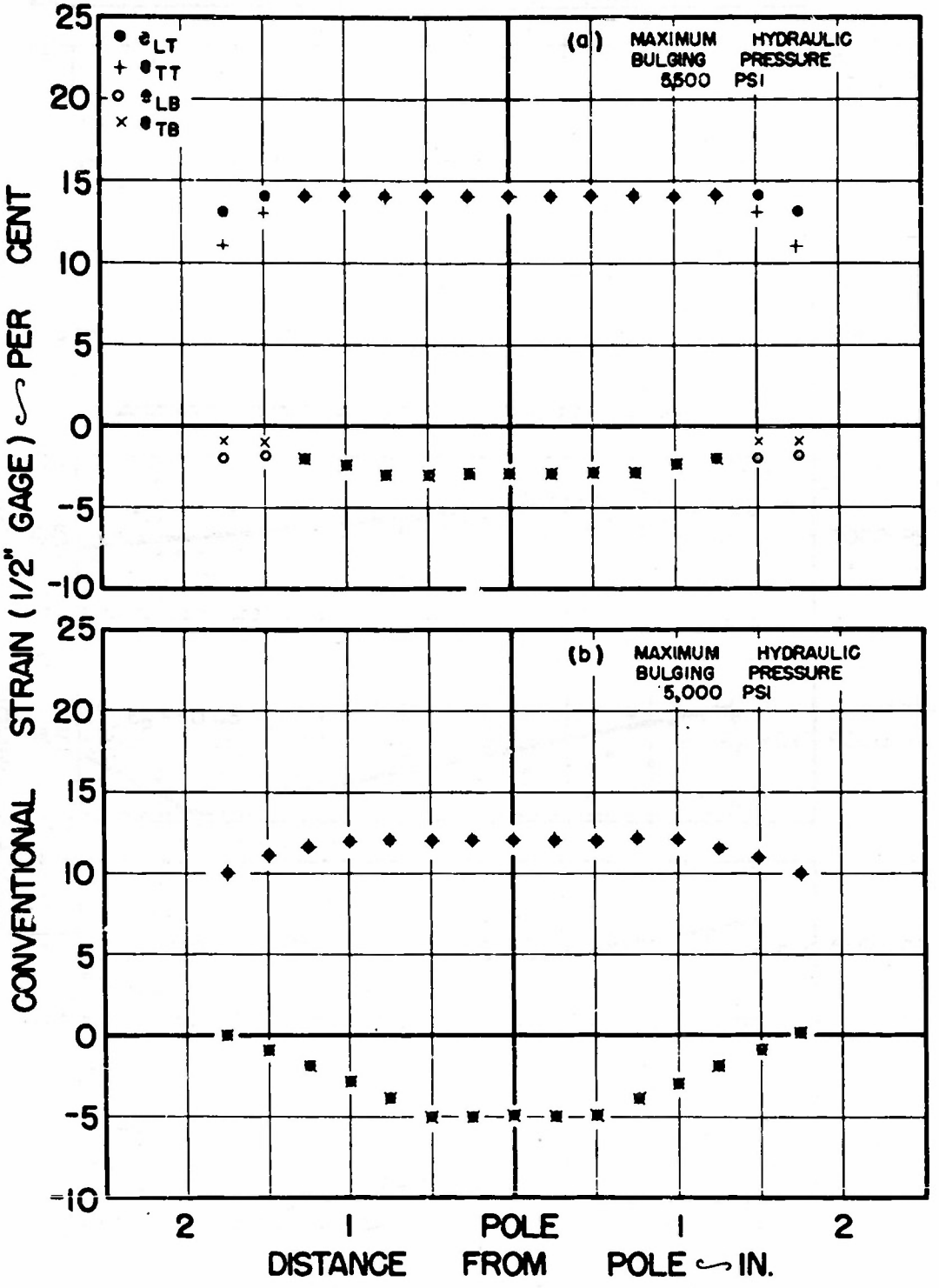

FIG. 7 : LONGITUDINAL AND TRANSVERSE STRAIN DISTRIBUTIONS FOR HYDRAULIC CIRCULAR BULGES OF 3/4" 2S-O ALUMINUM PLATE.

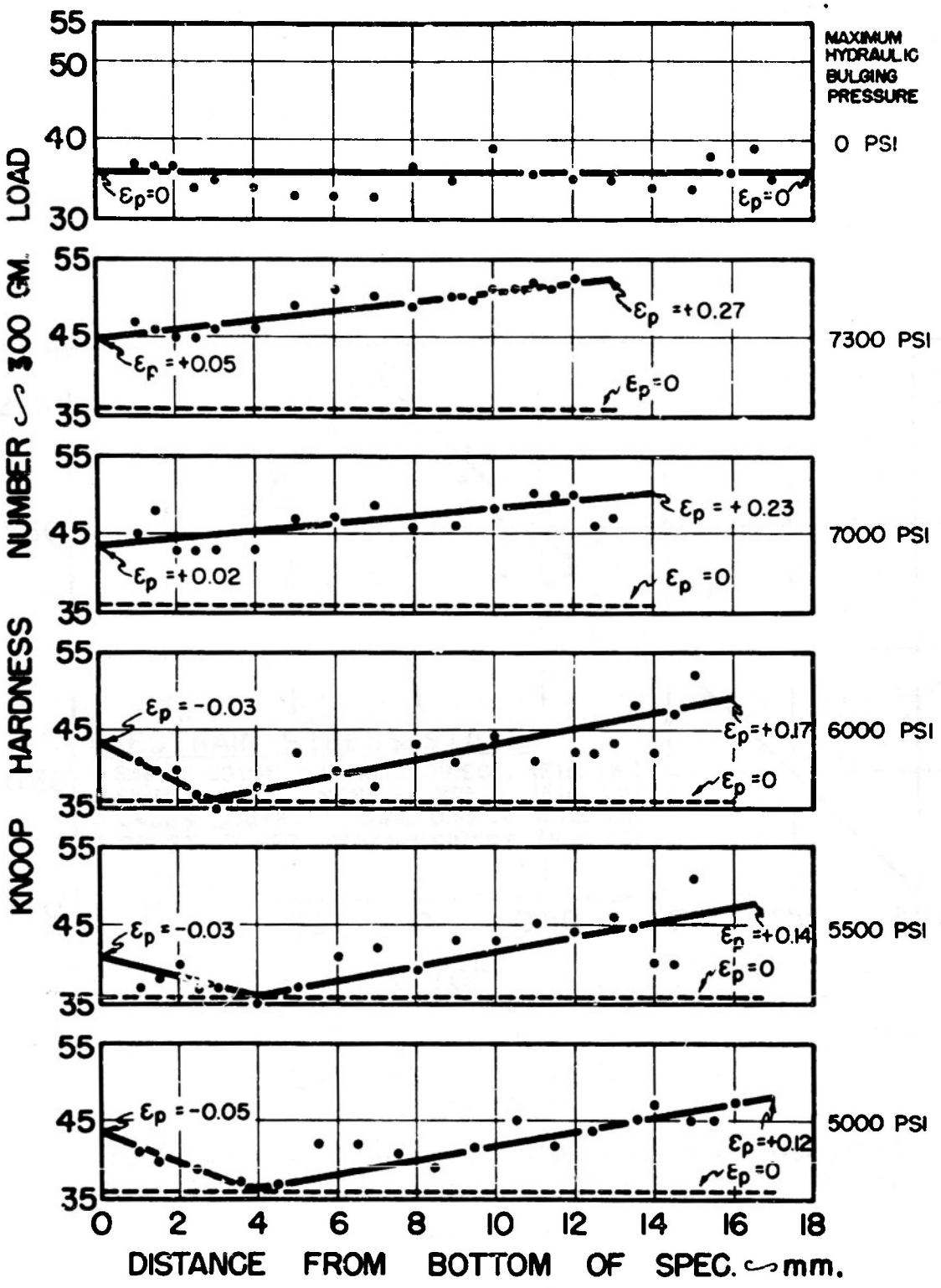

FIG. 8 : KNOOP HARDNESS TRAVERSES ALONG THE AXES OF 2S-O ALUMINUM TENSILE TEST SPECIMENS PRESTRAINED IN BIAXIAL TENSION.

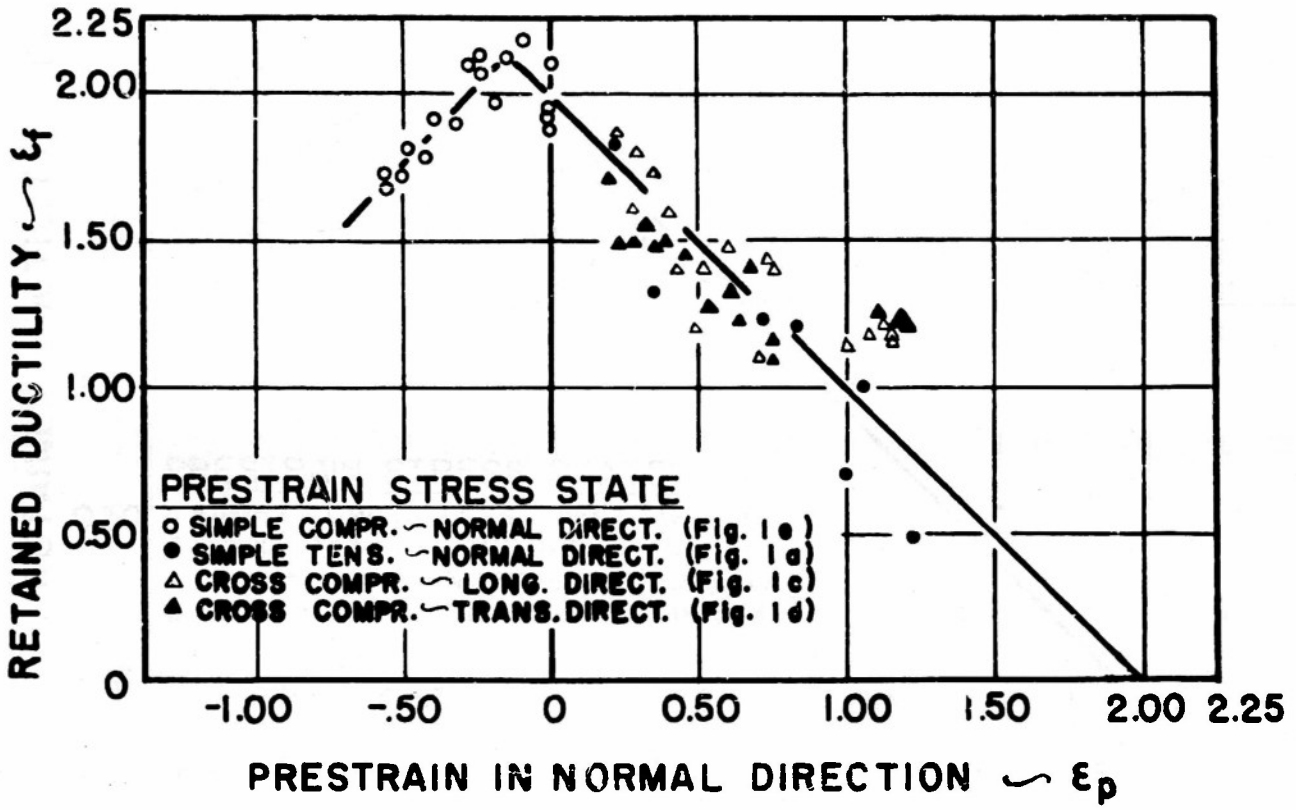

Fig. 9: EFFECT OF TENSILE ($\epsilon_p > 0$) AND COMPRESSIVE ($\epsilon_p < 0$) PRESTRAIN IN THE NORMAL DIRECTION OF ¾" THICK 2S-O ALUMINUM PLATE UPON THE RETAINED TENSILE DUCTILITY IN THE NORMAL DIRECTION FOR VARIOUS PRESTRAIN STRESS STATES.

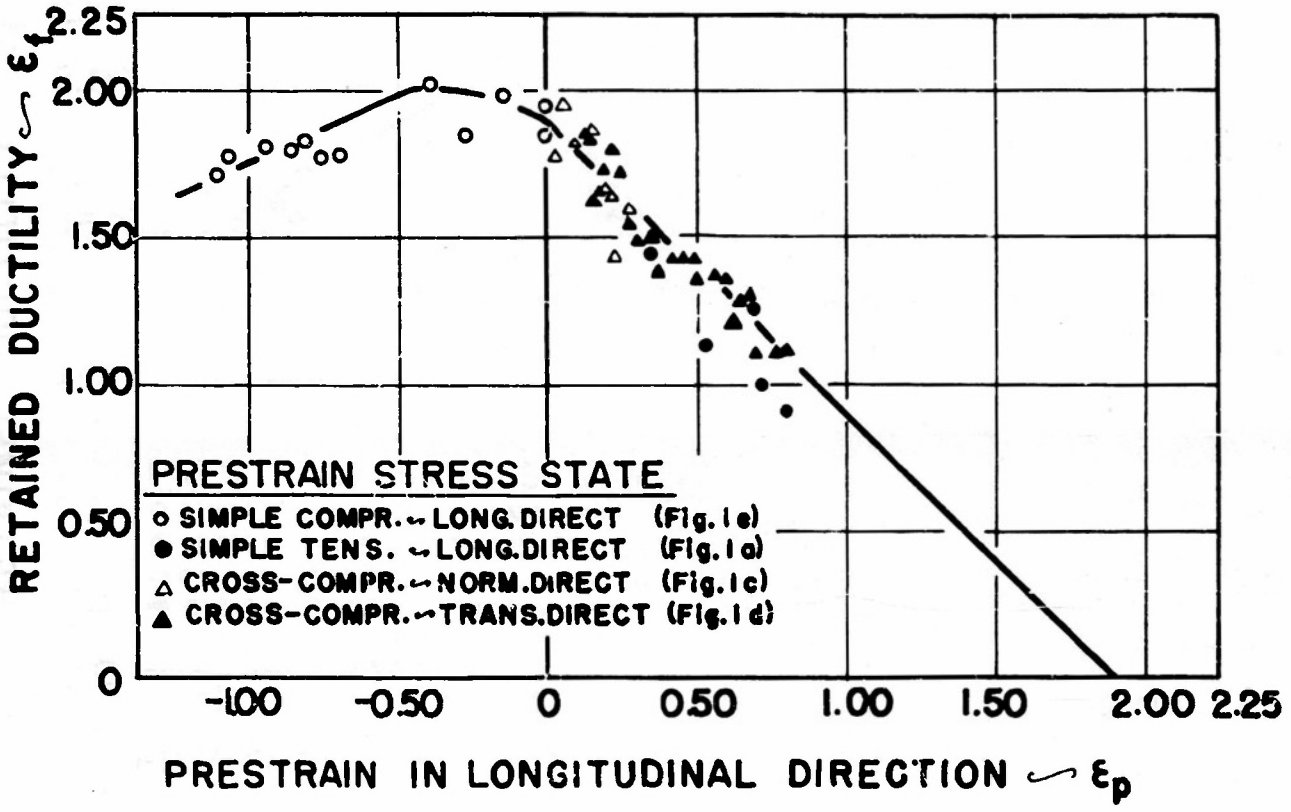

Fig. 10: EFFECT OF TENSILE ($\varepsilon_p > 0$) AND COMPRESSIVE ($\varepsilon_p < 0$) PRESTRAIN IN THE LONGITUDINAL DIRECTION OF 3/4" THICK 2S-O ALUMINUM PLATE UPON THE RETAINED TENSILE DUCTILITY IN THE LONGITUDINAL DIRECTION FOR VARIOUS PRESTRAIN STRESS STATES.

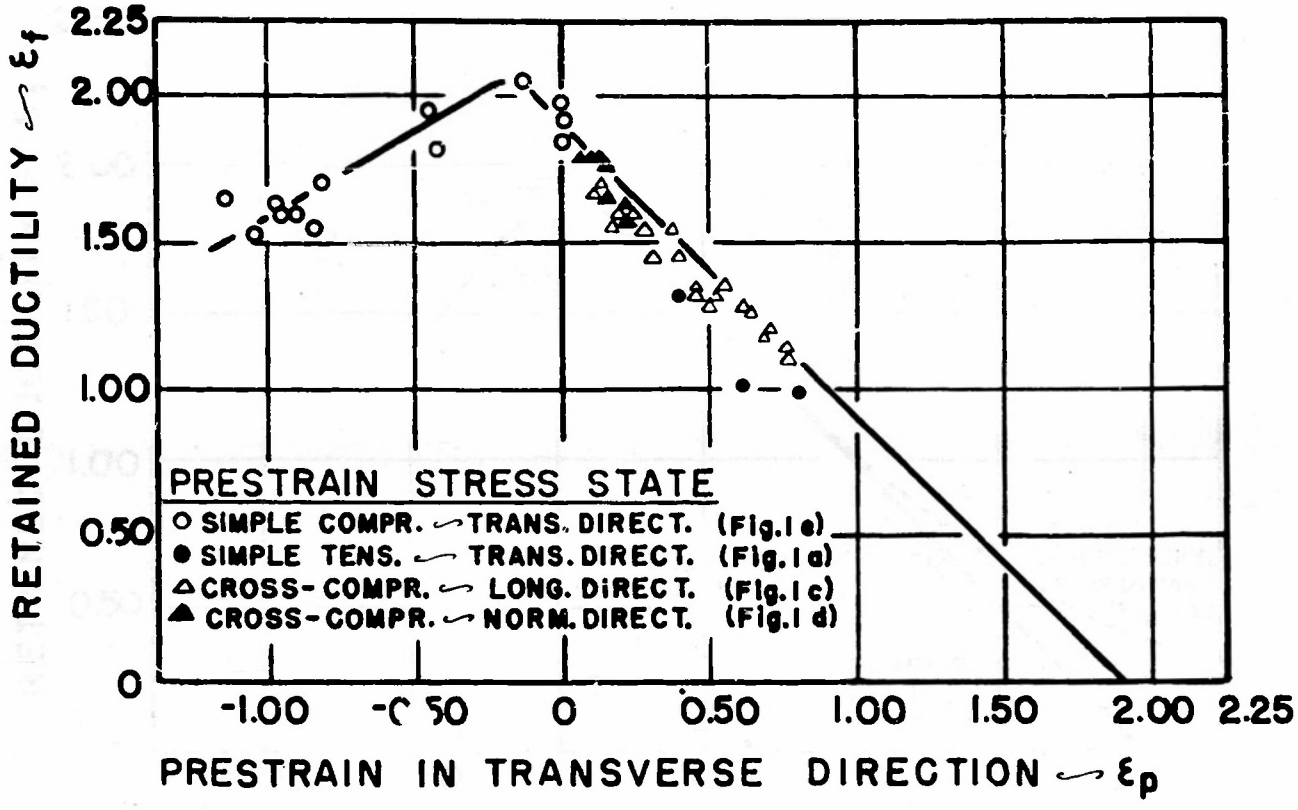

Fig. 11 : EFFECT OF TENSILE ($\varepsilon_p > 0$) AND COMPRESSIVE ($\varepsilon_p < 0$) PRESTRAIN IN THE TRANSVERSE DIRECTION OF 3/4" THICK 2S-O ALUMINUM PLATE UPON THE RETAINED TENSILE DUCTILITY IN THE TRANSVERSE DIRECTION FOR VARIOUS PRESTRAIN STRESS STATES.

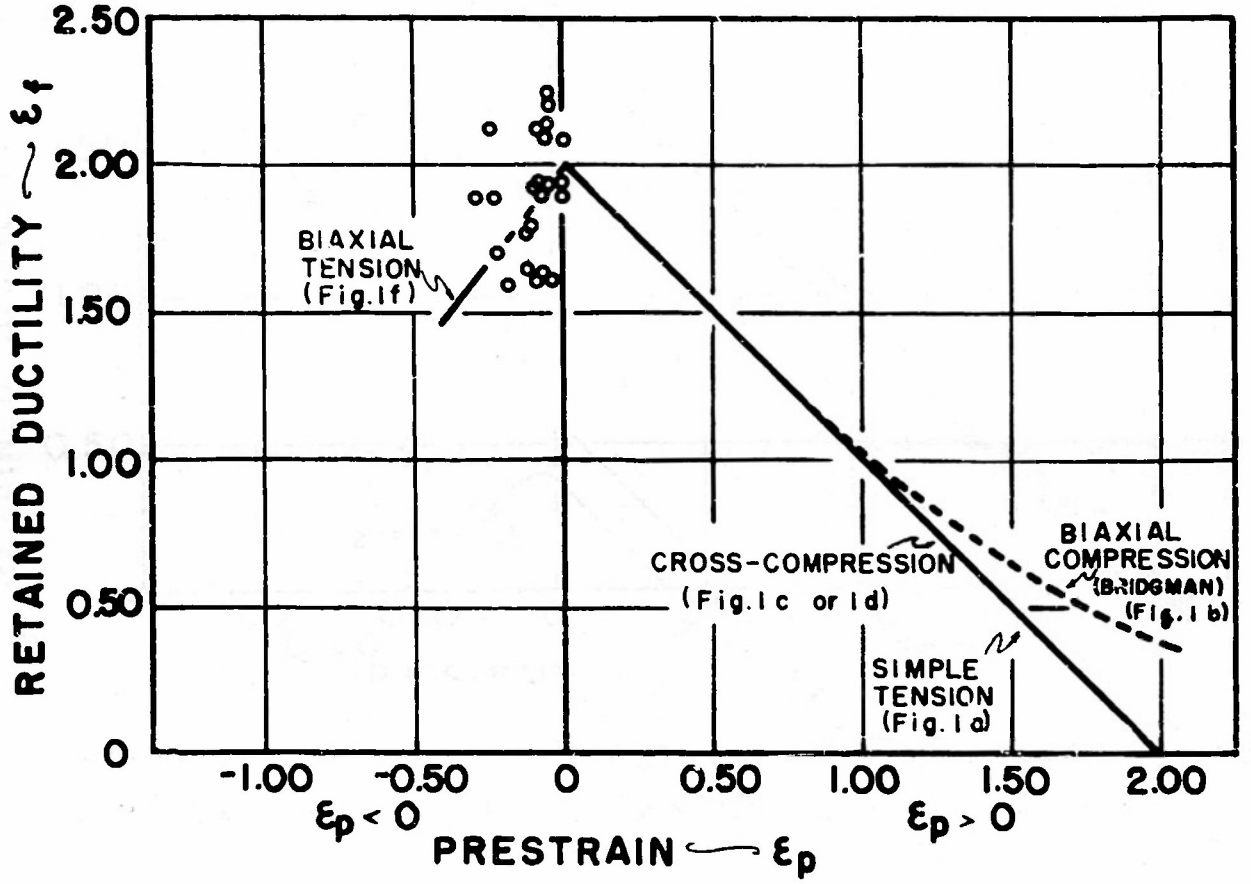

Fig 12: THE EFFECT OF PRESTRAIN IN BIAXIAL TENSION ($\varepsilon_p < 0$) AND IN BIAXIAL COMPRESSION ($\varepsilon_p > 0$)(SCHEMATIC AFTER BRIDGMAN) UPON THE RETAINED TENSILE DUCTILITY IN THE NORMAL DIRECTION OF 3/4" THICK 2S-O ALUMINUM PLATE.

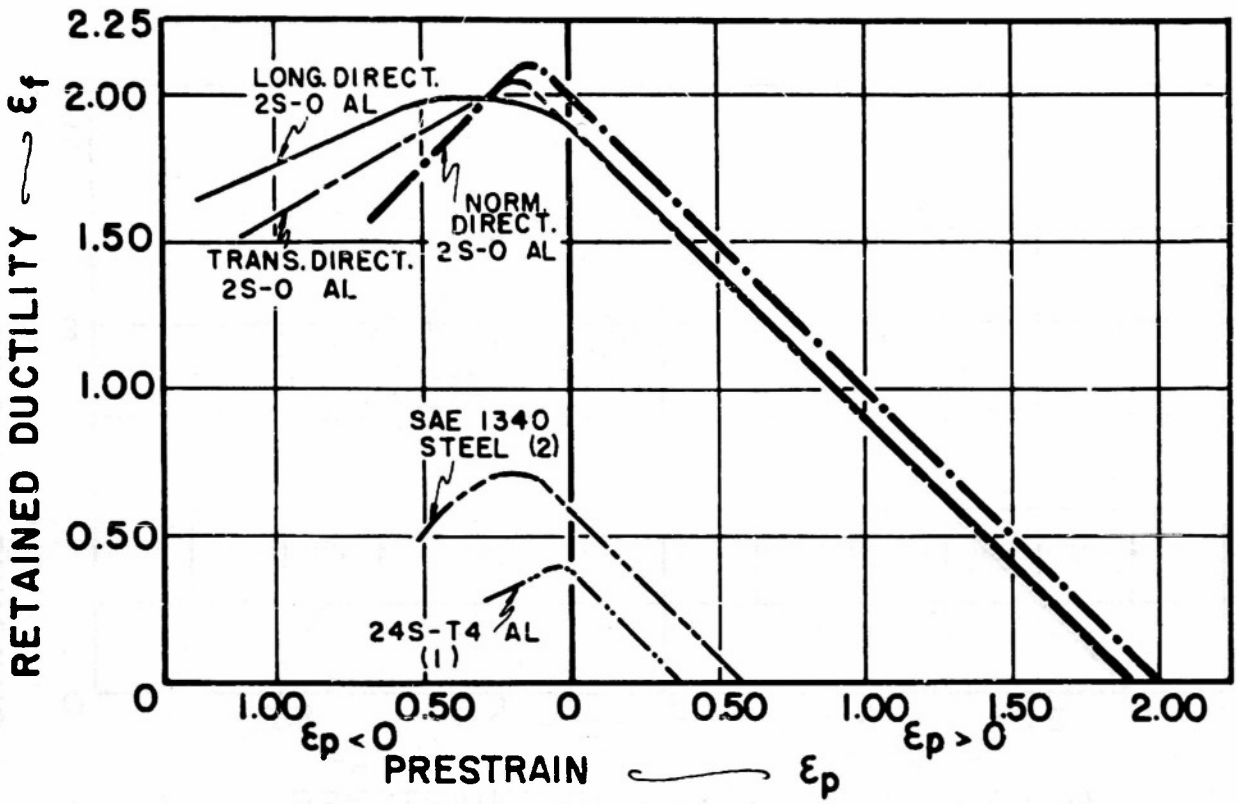

Fig.13: THE EFFECT OF PRESTRAIN IN SIMPLE COMPRESSION ($\varepsilon_p < 0$) OR IN SIMPLE TENSION ($\varepsilon_p > 0$) UPON THE RETAINED TENSILE DUCTILITY FOR 3/4" THICK 2S-O ALUMINUM PLATE FOR EACH OF THE THREE PRINCIPAL DIRECTIONS. THE PRESTRAIN DIRECTION WAS THE SAME AS THE DIRECTION OF THE SUBSEQUENT TENSILE TEST.

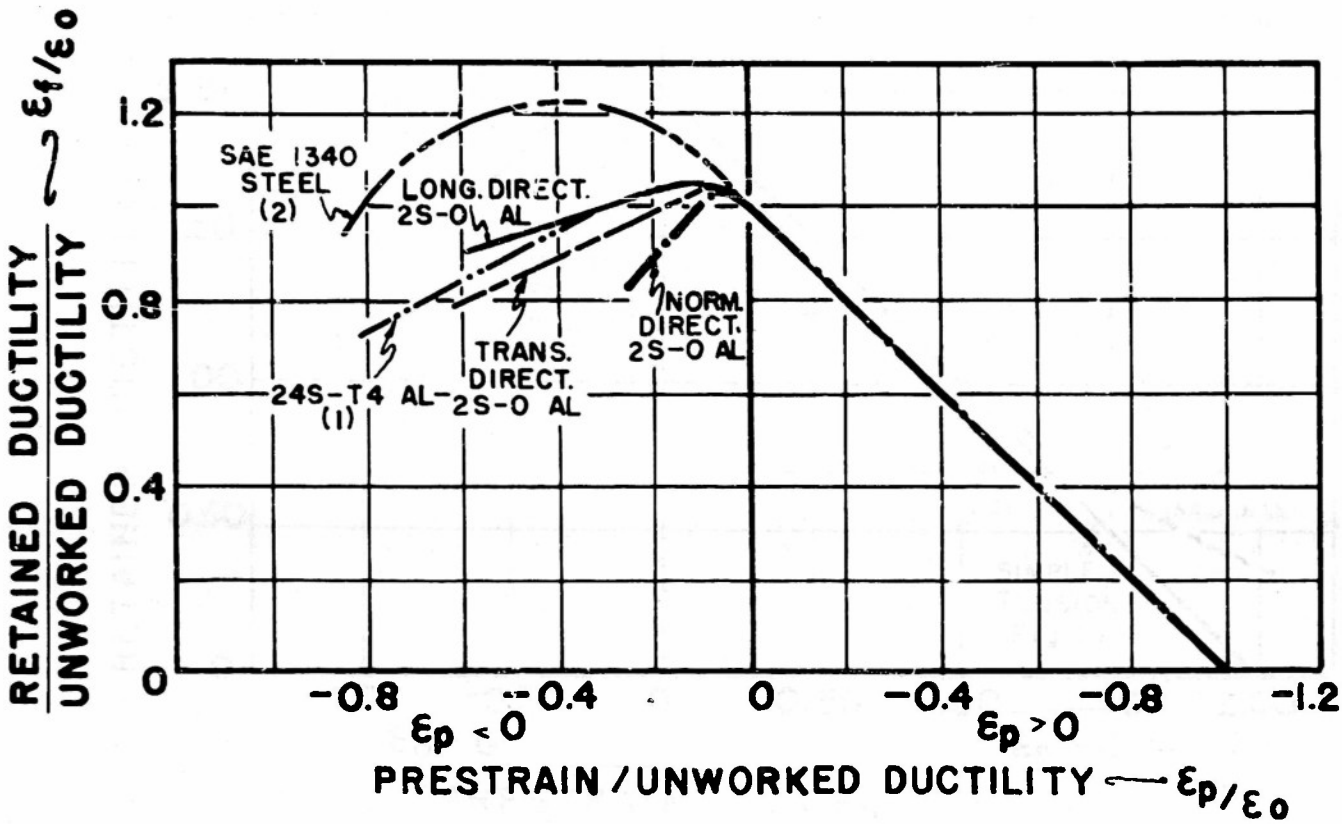

Fig. 14: THE EFFECT OF PRESTRAIN IN SIMPLE COMPRESSION ($\varepsilon_p < 0$) OR IN SIMPLE TENSION ($\varepsilon_p > 0$) UPON THE RETAINED TENSILE DUCTILITY FOR 3/4" THICK 2S-O ALUMINUM PLATE FOR EACH OF THE THREE PRINCIPAL DIRECTIONS. THE PRESTRAIN DIRECTION WAS THE SAME AS THE DIRECTION OF THE SUBSEQUENT TENSILE TEST.

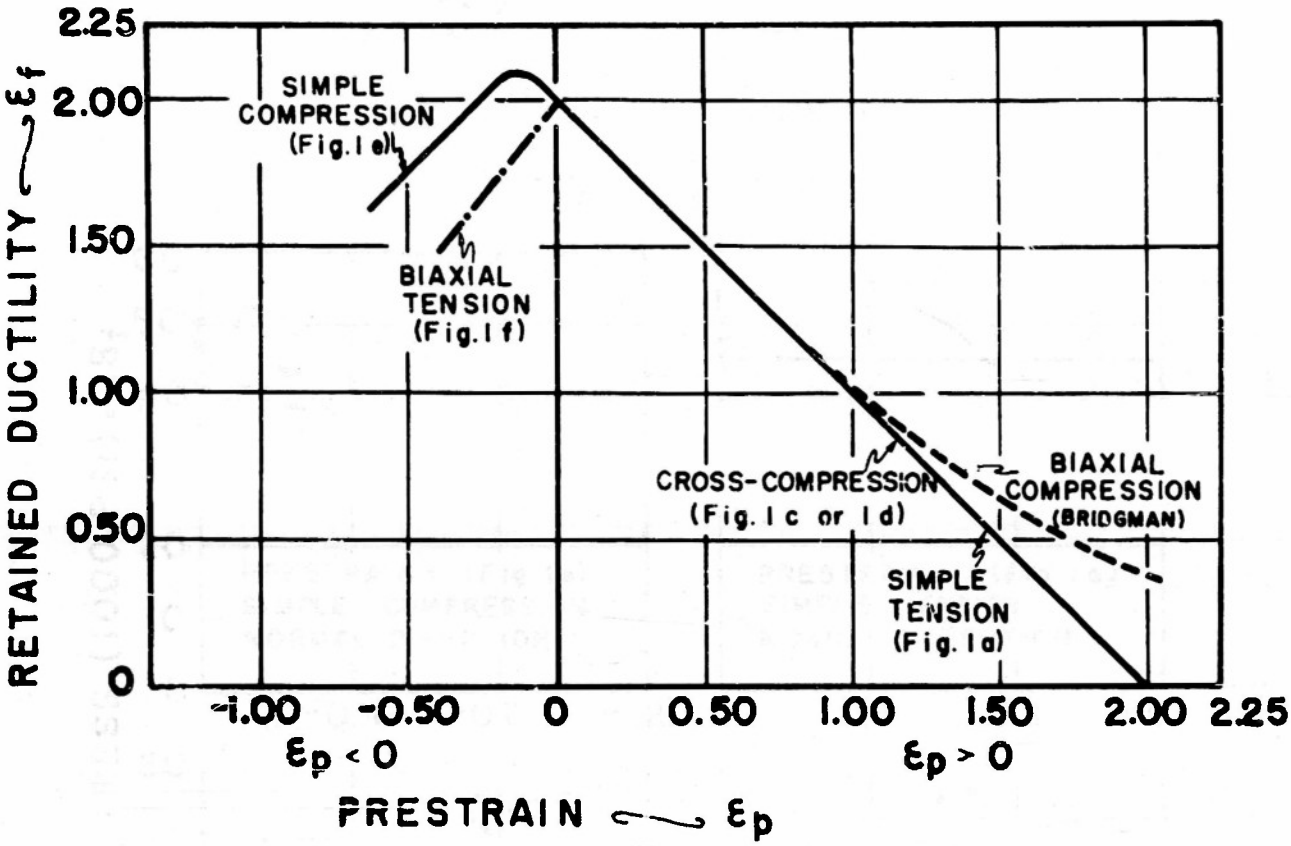

Fig.15: THE EFFECT OF PRESTRAIN STRESS STATE UPON THE RETAINED TENSILE DUCTILITY IN THE NORMAL DIRECTION OF 3/4" THICK 2S-O ALUMINUM PLATE. THE CURVE FOR BIAXIAL COMPRESSIVE PRESTRAIN IS SCHEMATIC AFTER BRIDGMAN (4).

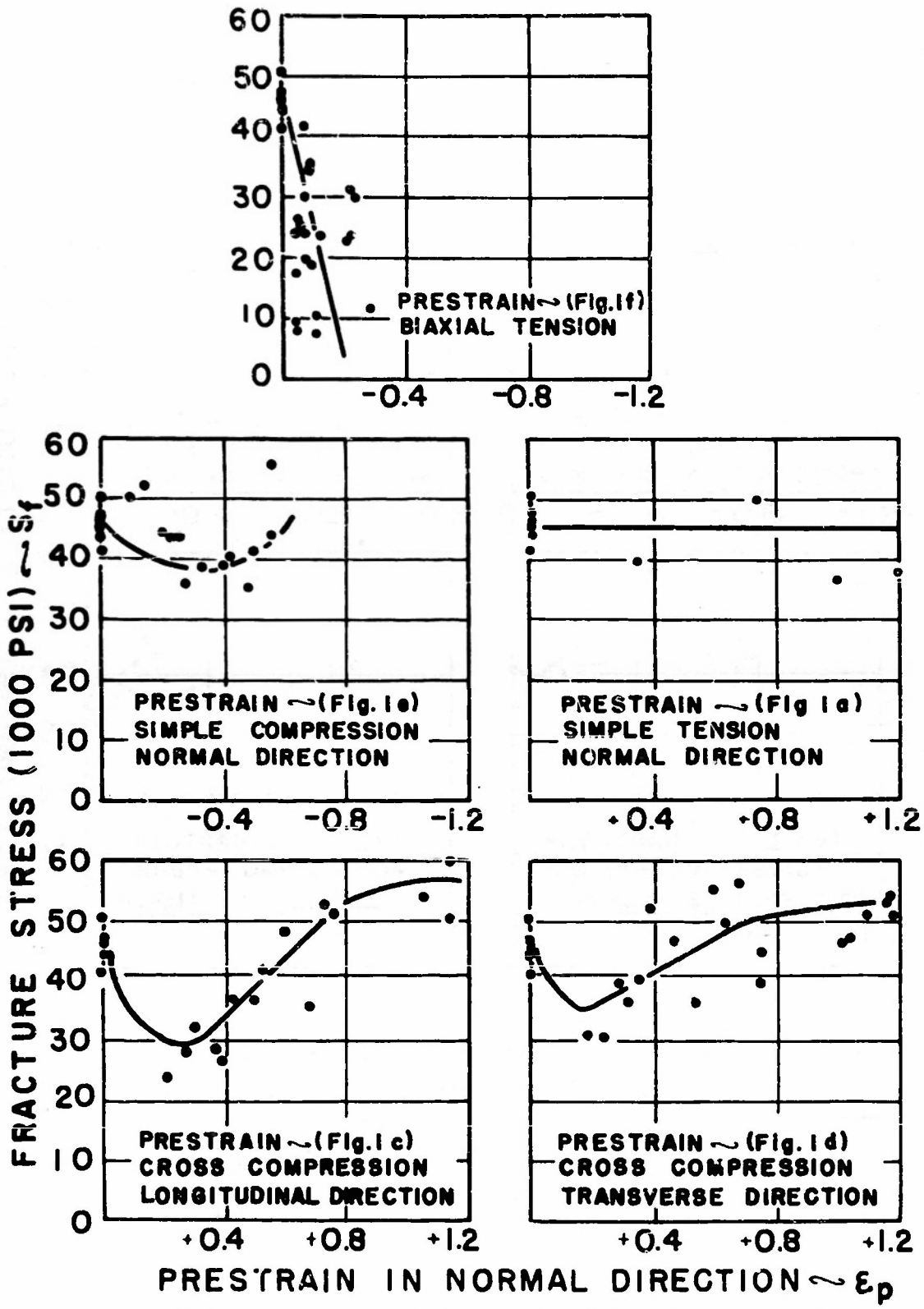

Fig.16: EFFECT OF VARIOUS PRESTRAIN STRESS STATES UPON THE TENSILE FRACTURE STRESS IN THE NORMAL DIRECTION OF 3/4 INCH THICK 2S-O ALUMINUM PLATE.

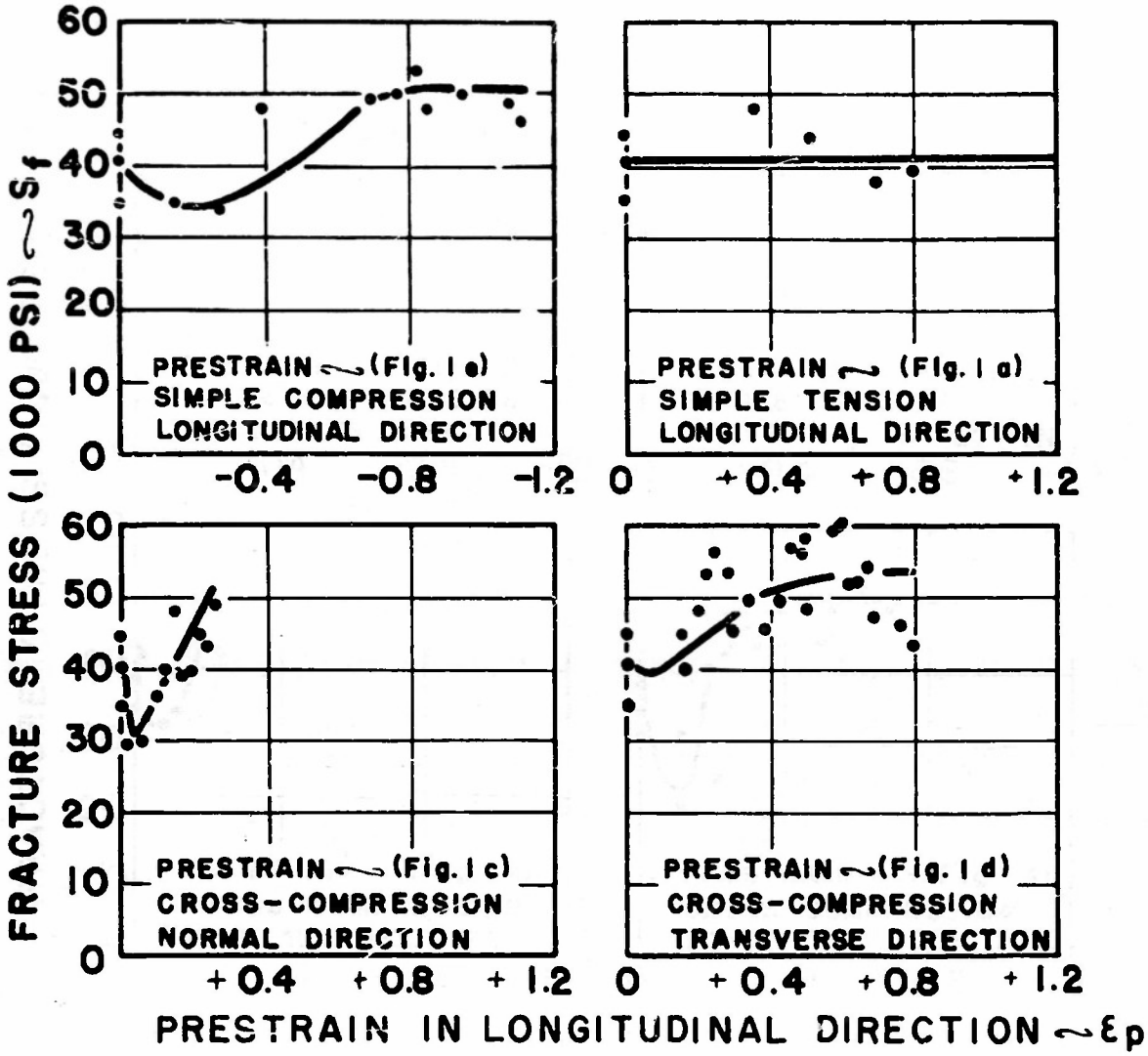

Fig. 17: EFFECT OF VARIOUS PRESTRAIN STRESS STATES UPON THE TENSILE FRACTURE STRESS IN THE LONGITUDINAL DIRECTION OF 3/4 INCH THICK 2S-O ALUMINUM PLATE.

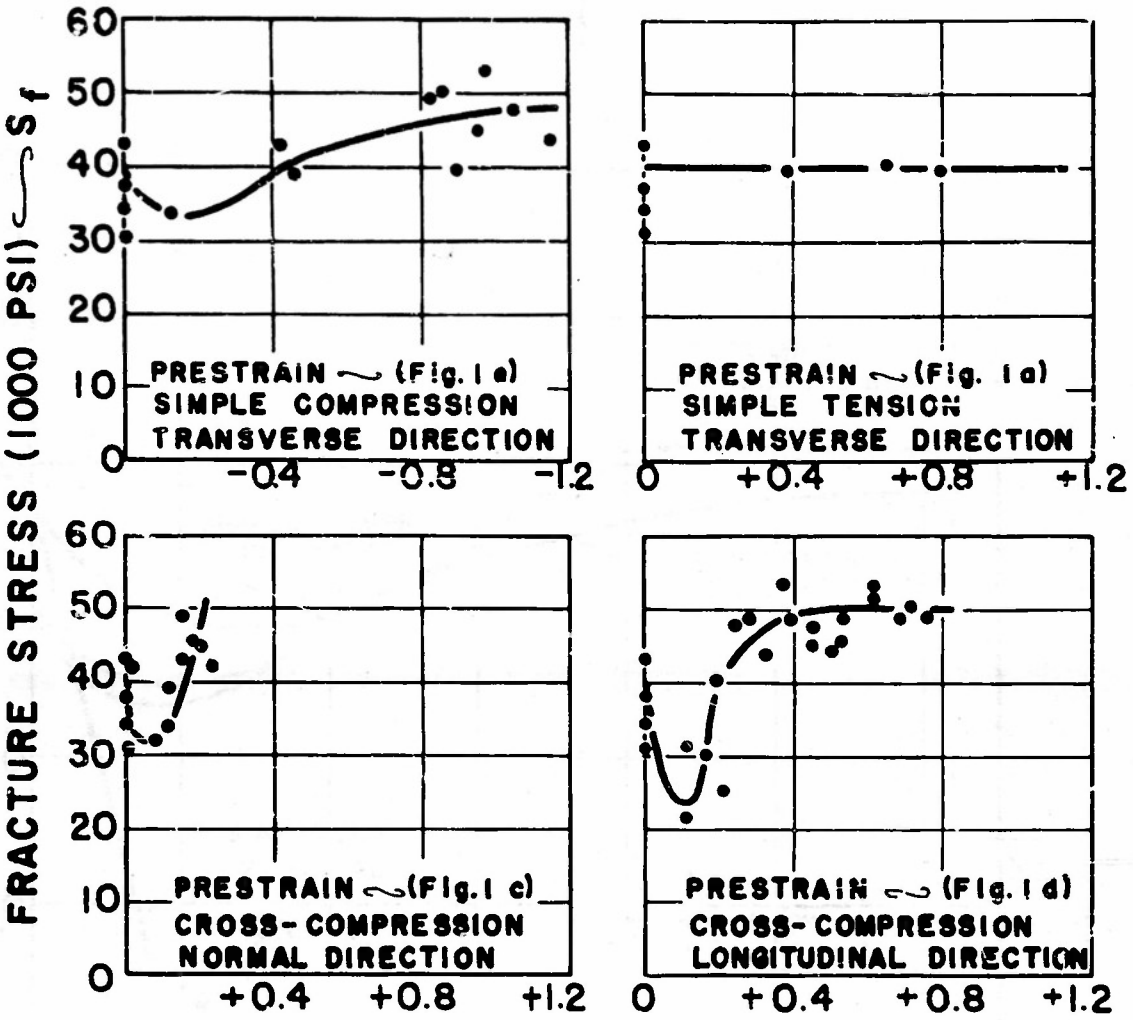

Fig.18: EFFECT OF VARIOUS PRESTRAIN STRESS STATES UPON THE TENSILE FRACTURE STRESS IN THE TRANSVERSE DIRECTION OF 3/4 INCH THICK 2S-O ALUMINUM PLATE.

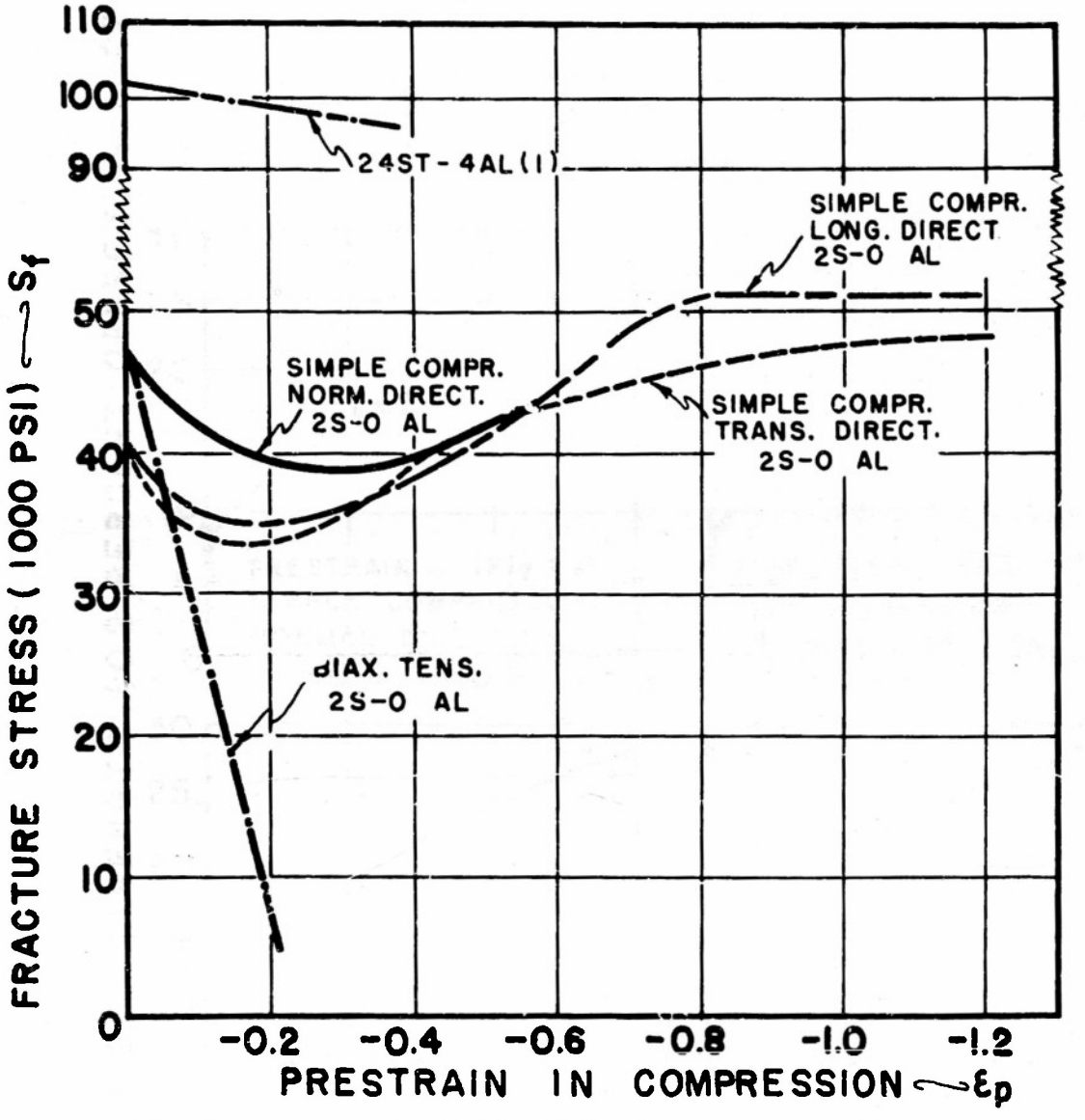

Fig. 19: COMPARISON OF COMPRESSIVE PRESTRAIN EFFECTS UPON THE FRACTURE STRESS IN TENSION OF 2S-O ALUMINUM FOR VARIOUS PRESTRAIN STRESS STATES AND PRESTRAIN DIRECTIONS.

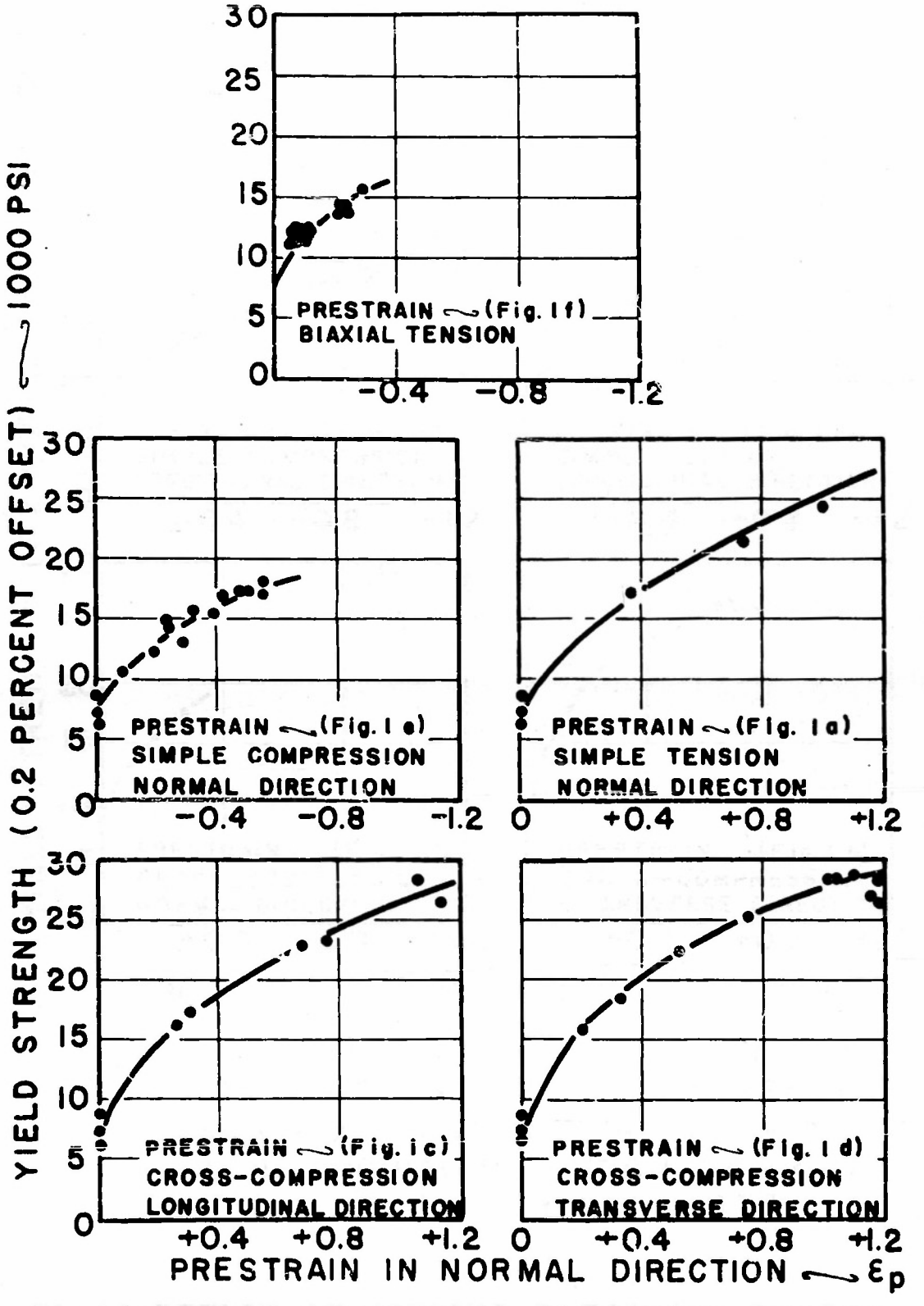

Fig.20: EFFECT OF VARIOUS PRESTRAIN STRESS STATES UPON THE YIELD STRENGTH(0.2 PER CENT OFFSET) IN TENSION IN THE NORMAL DIRECTION OF 3/4 INCH THICK 2S-O ALUMINUM PLATE.

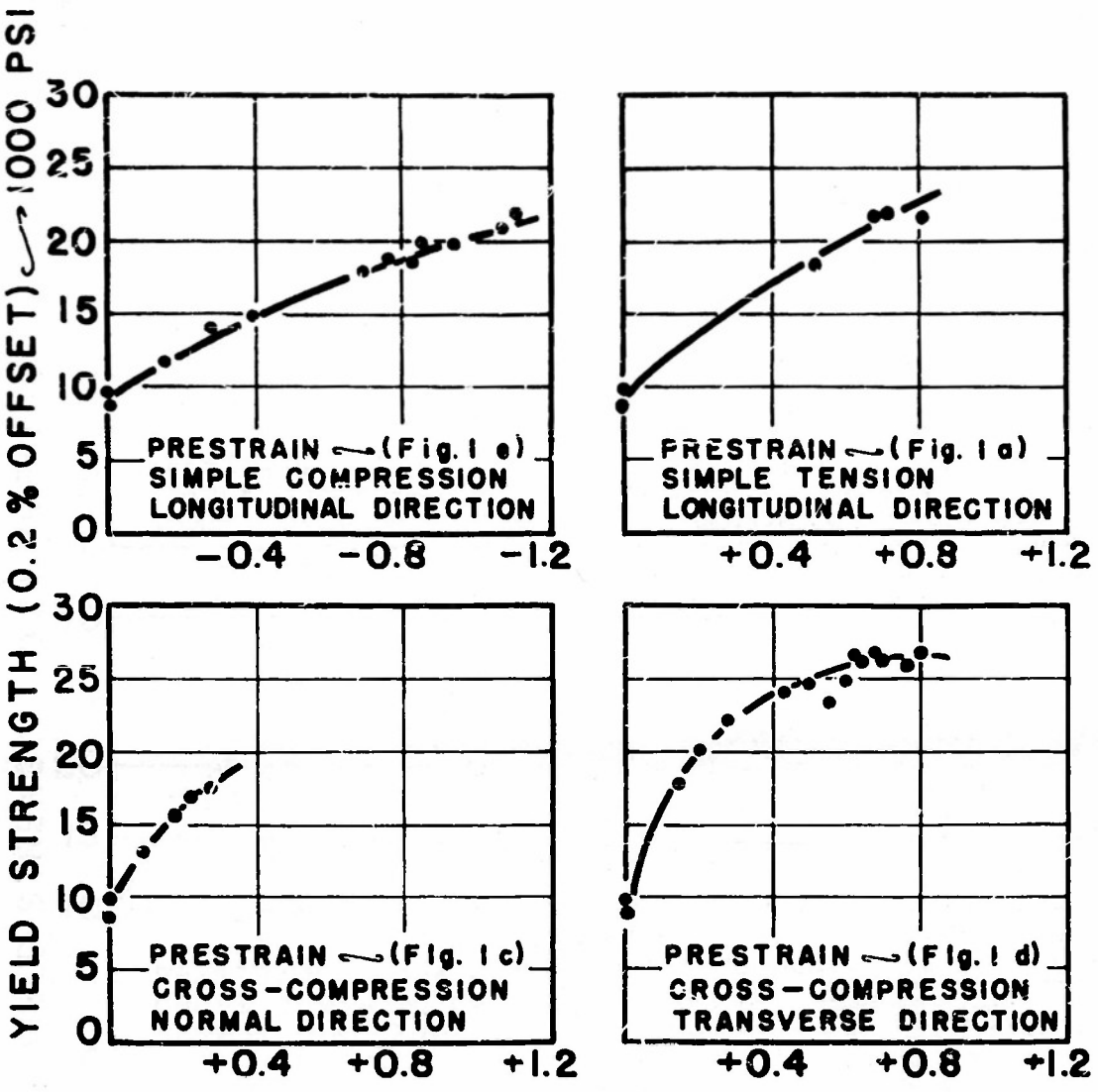

Fig 21: EFFECT OF VARIOUS PRESTRAIN STRESS STATES UPON THE YIELD STRENGTH (0.2 % OFFSET) IN TENSION IN THE LONGITUDINAL DIRECTION OF 3/4 INCH THICK 2S-O ALUMINUM PLATE.

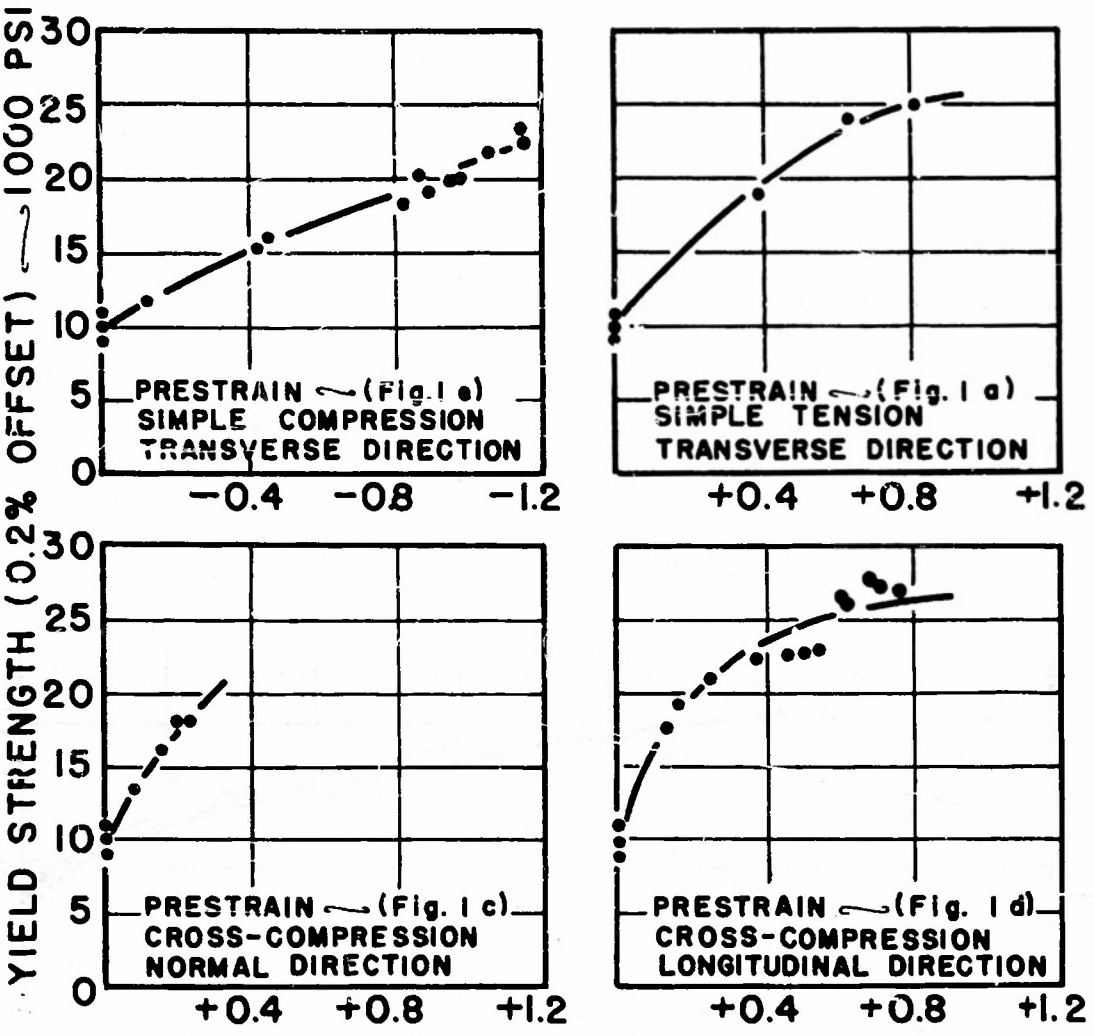

Fig. 22: EFFECT OF VARIOUS PRESTRAIN STRESS STATES UPON THE YIELD STRENGH (0.2% OFFSET) IN TENSION IN THE TRANSVERSE DIRECTION OF 3/4 INCH THICK 2S-O ALUMINUM PLATE.

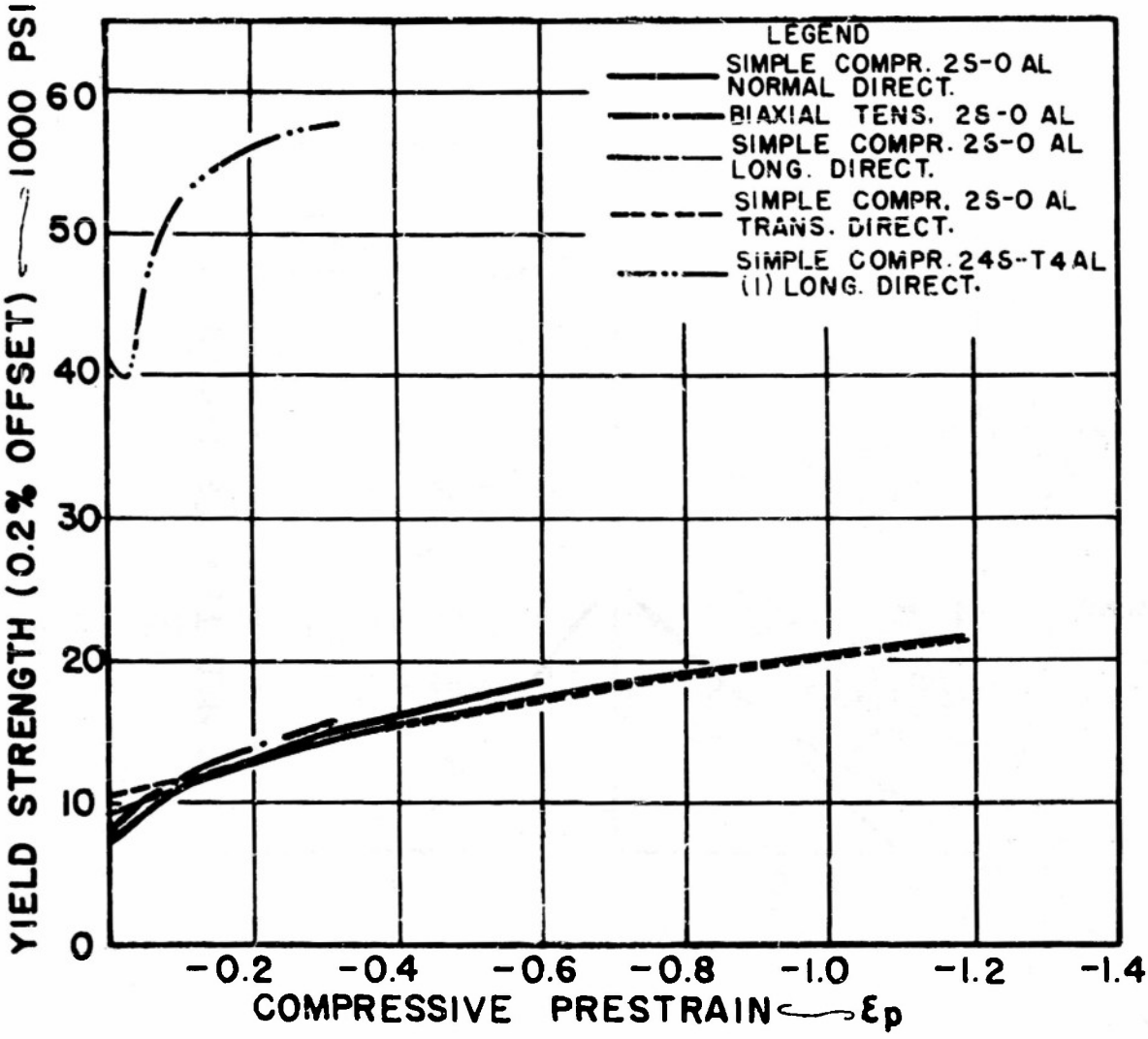

Fig. 23 : COMPARISON OF COMPRESSIVE PRESTRAIN EFFECTS UPON THE YIELD STRENGTH (0.2% OFFSET) IN TENSION FOR 3/4 INCH THICK 2S-O ALUMINUM PLATE AND 24S-T4 ALUMINUM (1) FOR VARIOUS PRESTRAIN STRESS STATES AND DIRECTIONS. THE PRESTRAIN DIRECTION WAS THE SAME AS THE DIRECTION OF THE SUBSEQUENT TENSILE TEST.

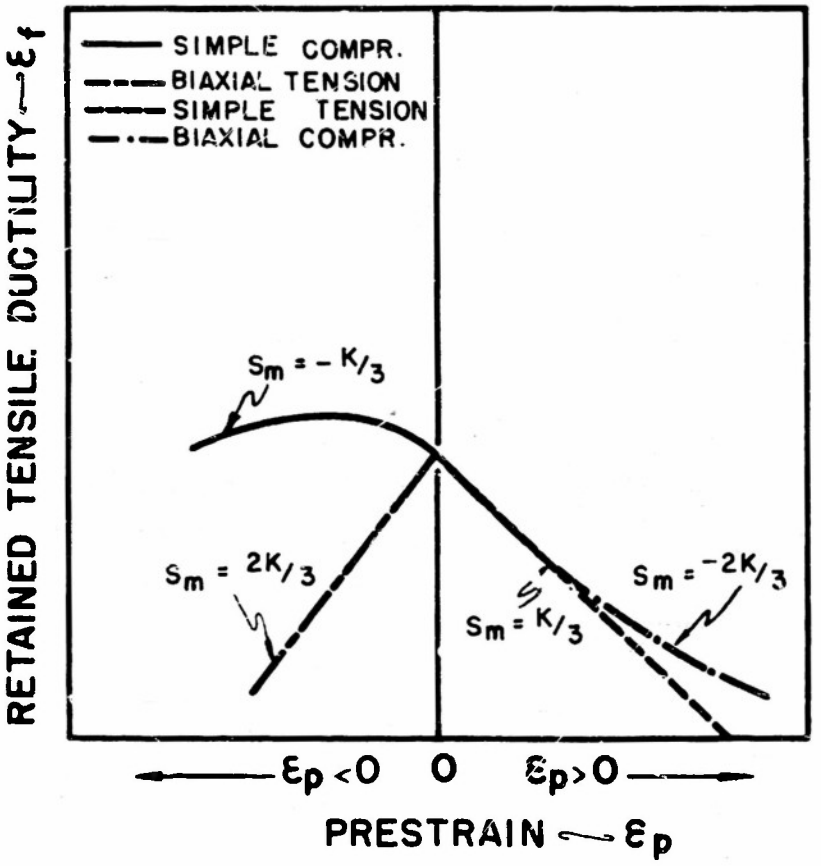

Fig. 24: SCHEMATIC REPRESENTATION OF RETAINED TENSILE DUCTILITY VERSUS PRESTRAIN FOR VARIOUS PRESTRAIN STRESS STATES FOR 2S-O ALUMINUM PLATE. THE PRESTRAIN DIRECTION IS THE SAME AS THAT OF THE SUBSEQUENT TENSILE TEST. THE MEAN STRESS (Sm) IS GIVEN FOR EACH PRESTRAIN STRESS STATE IN TERMS OF THE YIELD STRENGTH IN TENSION.